Title
Air pollutant exposure concentrations from cooking a meal with a gas or induction cooktop and the effectiveness of two recirculating range hoods with filters

Journal
Indoor Environments, 1(4)

ISSN
2950-3620

Authors
Li, Jiayu
Zhao, Haoran
Russell, Marion L
et al.

Publication Date
2024-12-01

DOI
10.1016/j.indenv.2024.100047

Journal-published version: Li et al. 2024. *Indoor Environments*, *1*(4), p.100047. doi.org/10.1016/j.indenv.2024.100047

Air Pollutant Exposure Concentrations from Cooking a Meal with a Gas or Induction Cooktop and the Effectiveness of Two Recirculating Range Hoods with Filters

Jiayu Li[1,2], Haoran Zhao[2,3], Marion L. Russell[2], William W. Delp[2], Alexandra Johnson[2], Xiaochen Tang[2], Iain S. Walker[2,3], Brett C. Singer[2,3,*]

[1] Center for the Built Environment, University of California, Berkeley, CA 94720

[2] Indoor Environment Group, Lawrence Berkeley National Laboratory, Berkeley, CA 94720

[3] Residential Buildings Group, Lawrence Berkeley National Laboratory, Berkeley, CA 94720

*Corresponding author.

Author Contributions

Jiayu Li: Data curation, Formal analysis, Validation, Visualization, Writing - original draft and review and editing; (ORCID: 0000-0002-5398-1151);

Haoran Zhao: Conceptualization, Data curation, Formal analysis, Investigation, Methodology, Supervision, Writing - review and editing (ORCID: 0000-0002-0802-0431);

Marion L. Russell: Formal analysis, Investigation, Methodology, Supervision, Writing - review and editing; ORCID: (0000-0002-7723-6746);

William W. Delp: Conceptualization, Data curation, Formal analysis, Visualization, Methodology (ORCID: 0000-0002-6071-2187);

Alexandra L. Johnson: Investigation (ORCID: 0000-0002-4641-1556);

Xiaochen Tang: Formal analysis, Writing - original draft (ORCID: 0000-0002-6435-6116);

Iain S. Walker: Conceptualization, Funding acquisition, Project Administration, Writing - review and editing; (ORCID: 0000-0001-9667-1797)

Brett C. Singer: Conceptualization, Formal analysis, Funding acquisition, Methodology, Project Administration, Supervision, Visualization, Writing - original draft and review and editing (0000-0001-5665-4343)

ABSTRACT

This study compares air pollutant concentrations resulting from cooking with gas or induction cooktops, with or without either of two recirculating range hoods with filters. A meal of pasta, plant-based "meat" sauce and stir-fried broccoli was cooked three times for each cooktop and hood combination in a 158 m^3 room. Time-resolved measurements were made of nitrogen oxides, carbon dioxide, size-resolved particles, and speciated volatile organic compounds (VOCs) during cooking and 30 minutes after cooking. Cooking with induction used half as much energy and produced no discernible NO_X and significantly reduced ultrafine particles (UFP, diameter < 100 nm) and CO_2 compared to gas cooktops. Induction produced statistically higher $PM_{2.5}$ when calculated using size-resolved particle measurements from one pair of instruments, but the difference was not discernible when calculating from another pair. With gas cooktops, roughly half of the $PM_{2.5}$ was in particles smaller than 0.3 µm and thus below the lower quantitation threshold for many optical particle instruments; optical devices may thus substantially under-report $PM_{2.5}$ from gas cooking. VOCs did not significantly differ between gas and induction. Both recirculating range hoods substantially reduced all particle sizes when cooking with either fuel, and the reductions were larger for gas cooking. One of the range hoods also substantially lowered some of the VOCs.

KEYWORDS

Fine particulate matter; Nitrogen dioxide; Personal exposure; Ultrafine particles; Volatile organic compounds

HIGHLIGHTS

1. Measured air pollutants from cooking a simple meal with gas or induction cooktop.
2. Induction used 50% less energy, emitted no NO_X and fewer ultrafine particles.
3. Cooking <u>this</u> meal with induction likely emitted more $PM_{2.5}$.
4. Half of the gas-cooking $PM_{2.5}$ was under the optical sensor threshold of 0.3 µm.
5. Both recirculating range hoods with filters substantially reduced particle levels.

INTRODUCTION

Cooking produces air pollutants that can result in substantial exposure and health hazards within homes. Pollutants can be generated by the cooking appliance and also by the cooking process. Gas burners emit nitrogen oxides (NO_X), including nitrogen dioxide (NO_2) and nitrous acid (HONO) [1–8] and also emit ultrafine particles (UFPs) [3,6,9] – all at levels that can detrimentally impact indoor air quality (IAQ) when not removed by adequate kitchen exhaust ventilation. Combustion also produces water vapor, which can contribute to humidity problems under some circumstances. Electric resistance cooktops also produce UFPs [3,10,11] independent of cooking; and the limited available evidence suggests that this occurs much less with induction cooktops [10]. UFPs are also produced from heating pans to high temperatures, which is thought to be caused by volatilization of condensable organics and detergents that have been deposited on the pans previously [12]. And while properly functioning, modern gas burners may not produce carbon monoxide (CO) in substantial quantities, discernibly higher CO concentrations have been reported for groups of existing homes using gas vs. groups using electric burners [5].

Cooking with both gas and electric cooktops generates airborne particles that vary widely in size and composition [13]. Several studies have reported comparisons of fine particulate matter ($PM_{2.5}$) resulting from gas vs. electric cooking. An analysis of photometer-based, time-resolved particle measurements in Canadian homes with electric (n=103) or gas (n=29) cooking estimated that $PM_{2.5}$ source strengths were approximately twice as high with gas vs. electric cooking [14]. The authors noted that this result was directionally consistent with the findings of a controlled cooking study by Zhang et al. [15], but counter to Olson and Burke [16] who reported higher PM emissions from electric cooking in homes. Additionally, Buonanno et al. [17] reported that cooking bacon on gas stoves emitted more airborne particles by number but fewer by surface area and mass, compared to electric stoves. Reviewing these and other studies, Torkmahalleh et al. [18] concluded that the literature definitively shows that “particle emission rates” are higher with gas compared to electric cooking; but they did not specify whether their assessment referred only to the number of particles or also to mass. In a recent study, Johnson et al. [19] reported that standardized cooking of beef burgers (one at a time) on an electric resistance cooktop resulted in 2 to 3 times higher airborne particulate matter concentrations sampled at 17.8 cm above the burger, compared to the same cooking on a gas or propane burner. They attributed the differences to greater pan surface temperature fluctuations when using the electric resistance cooktop.

Several approaches are available to reduce pollutant exposure from cooking. Shifting from gas to electric cooking cooktops reduces emissions of NO_X and UFPs and the likelihood of CO emissions. A recent study by Daouda et al. [20] reported substantially larger reductions in New York City apartments that had their gas stoves replaced with an induction stove (by random selection) compared to controls that continued to use their gas stove. Use of a venting range hood when cooking with any fuel can substantially remove pollutants before they mix into the room, and thus reduce exposure [6,21–26]. Modifying cooking procedures also can reduce pollutant emissions [18,24]. While exhaust ventilation at the source can be an effective control, there are many homes that do not currently have an exhaust ventilation duct configured to draw from the area above or near the stove. And some homes—particularly apartments in multifamily buildings—may not be able to add kitchen ventilation due to cost and/or building codes that limit the locations of exhaust vents. Also, most recirculating hoods do not include any pollutant removal technology, with users perceiving that they are less effective. A nationally representative survey of Canadian households found almost 90% had a range hood or microwave over their cooktop and about two-thirds vented to outdoors [27]. Respondents reported (with statistical discernibility) that the recirculating hoods performed less well at removing grease, odor, smoke, heat and moisture; and they were used less often (ibid). Some recirculating range hoods include filters that are primarily marketed for odor removal and one limited study reported that a hood with a carbon filter showed some effectiveness for NO_X and $PM_{2.5}$ also [28]. Recently, Wojnowski et al. [29] evaluated the performance of recirculating range hoods with active carbon filters in minimizing exposure to

VOCs and found that the filters were generally effective in removing odorants such as trimethylamine and acetic acid but struggled with alcohols. For homes that don't have and cannot easily add a ventilation duct from the kitchen area, recirculating hoods with filters could, if effective, facilitate pollutant removal directly from the cooking area.

While some of the benefits of shifting from gas to induction are certain (e.g., reducing NO_X and UFP from gas combustion), the effect of the fuel on overall pollutant emissions from cooking has not been assessed in a controlled manner. One rational way to approach this is to cook the same dish(es) using the same pots and similar heat transfer to the food to produce a similar finished product while using either gas or induction cooktops.

The first goal of this research was to develop and apply an approach to explore potential differences in pollutant emissions from cooking with gas or induction cooktops. The second goal was to conduct a preliminary investigation of the potential air quality benefits of recirculating range hoods with filters for particulate and/or gaseous pollutants. To advance these goals, we developed scripted procedures to cook a simple meal with several cooking activities, implemented on a gas and an induction cooktop. The meal was cooked three times with each cooktop, first without the use of a recirculating range hood, then again with three replicates to study the impact of each of two different range hoods with pollutant filters.

MATERIALS AND METHODS

Facility

We conducted experiments in Cell 3A of the FLEXLAB research facility at Lawrence Berkeley National Laboratory (www.flexlab.com). The experimental space is a rectangular room measuring 6.1 m (north-south) by 9.3 m (east-west), providing a floor area of 57 m^2. A panelized hanging ceiling at 2.7 m height delineates a 158 m^3 room. The full volume of the cell, including the space above the ceiling, is approximately 237 m^3.

We built a structure that allowed easy swapping of the gas and induction cooktops. The idle cooktop during each experiment was stored on an adjacent structure or cart. The configuration is shown in Figure S1 and detailed in Supporting Information.

Two 76 cm wide cooktops were used in the experiments. The gas cooktop (Whirlpool Model W3CG3014XB) was fueled with ultra-high purity methane (99.99%), and flow was monitored using an Alicat M-series mass flow meter. Power use by the induction cooktop (Empava Model Empv-30ec02) was monitored by the dedicated circuit monitoring of the FLEXLAB facility.

Two recirculating range hoods were selected to meet the following criteria: wall-mounted or under cabinet (not island); included an activated carbon bed or filter with sufficient depth or mass to suggest potential effectiveness for reducing volatile organic compounds (VOC); included a filter that could plausibly remove some fine particulate matter; had a setting that provided at least 100 $L \cdot s^{-1}$ of airflow at 2 sone or less; and the hood and filter and any required adapter kit was available for US$2000 or less. Candidate hoods were identified through online product searches and queries to manufacturers and experts within the industry. We selected two hoods for pilot testing, which are henceforth identified as Hood A and Hood B. A production unit of each hood was provided by the manufacturer from normal supply chain stock.

Both hoods had grease removal technology at the air inlet. Hood A employed an engineered baffle system with a curved plate over each of the two 20.3 cm diameter inlet fans designed to achieve grease droplet removal by impaction. The air inlet of Hood B was covered by a 50.8 cm wide by 17.1 cm deep multi-layered expanded metal screen to separate and collect grease droplets. For odor control, both hoods utilized carbon-based adsorption strategies. The outlet of Hood A, downstream of the fan, was a 20 cm diameter × 16.5 cm long cylindrical metal screen cartridge lined with a ~5 cm thick open cell foam pad (total mass of 126 g) coated with activated carbon. For Hood B, above the grease screen and upstream of the fan, there were two pleated filters that were designed to remove both fine particles and odors using multilayer laminated media containing a mix of activated charcoals. These filters were each 4.4 cm deep with pleats spaced approximately 1 cm apart and a total mass of 246 g. The media descriptions were provided by the technical staff of the range hood manufacturers. The retail price of each hood was determined by a search of online retailers in December 2023. The price for Hood A (in $US) was $849 and the odor filter was $115. The price for Hood B was $1499 and the recirculation kit was $115. The combined odor and particle filter used in Hood B was a product sold in Europe but not in the U.S. at the time, with a list price of €99.

For the experiments, each hood was installed such that the bottom plane was 57 cm above the grates and 61 cm above the plane of the gas cooktop and the induction cooktop. For experiments without range hood use, there was always a range hood installed above the cooktop. Each hood was operated on its second lowest setting. For Hood A, this produced an in-situ measured airflow of 527 $m^3 \cdot h^{-1}$ with a sound pressure level of 52 dBA and used 136W. Hood B in-situ airflow was 415 $m^3 \cdot h^{-1}$ with a sound pressure level of 62 dBA and power consumption of 260W. The background sound pressure level in the chamber during these measurements (with all equipment turned off) was 37 dBA.

Cooking and experimental procedures

The cooking procedure regulated timing, heat settings, and prescribed pictures and weighing the food at specific stages, as detailed in Supporting Information 2. Closely similar cooking conditions were achieved on the gas and induction cooktops by providing similar heat delivery rates to the contents of each pot. We identified the burner settings needed to do this by conducting experiments in which we filled each pot with a specified quantity of water and manipulated the settings on each cooktop to achieve nearly identical heating rates for the water in the pot. Further details are provided in Supporting Information 3.

Cooking procedures included the common activities of cooking pasta in boiling water; sauteing a plant-based meat alternative (Impossible burger) in olive oil; adding the sauteed "meat" to a tomato-based sauce and heating; stir-frying broccoli in corn oil over medium to high heat; and mixing the plant-based meat sauce, broccoli and pasta together. The sequence is presented in Figure 1. Before cooking, all the ingredients (water, plant-based meat, salt, oil, tomato sauce, corn oil, spaghetti, and broccoli) were precisely weighed. All cookware was induction-ready, multi-ply stainless steel, and the frying pan had a non-stick coating (specific products identified in the SI). The same cookware was used for gas and induction cooking.

Throughout the cooking period, two burners were utilized. The right-back burner was dedicated to boiling water and then cooking spaghetti in a 10.4-L stockpot with 28 cm diameter base. This was done with ~4.4 standard liters per min (SLPM) methane flow on the gas burner and ~1500W (Level 7) on the induction element. The left front burner was used first to fry the meat and then heat the meat with sauce using ~2.4 SLPM methane on the gas burner and ~640W (Level 6) on the induction element. This cooking occurred in a cylindrically shaped 1.9-L pot with 17.8 cm diameter base and 10.2 cm height. When the plant-based meat sauce was fully heated, it was covered and moved to the back left of the cooktop. The front left burner was then used to stir-fry the frozen broccoli florets in a 23 cm diameter frying pan with a gas flow of ~3.3 SLPM (estimated based on a total measured flow of 7.6 SLPM for this pan and the pasta pot). The target power setting for the induction to match the energy delivered to the contents of the pan was ~1200W. However, the closest available power settings for the left front element were 1500W on level 8 and 750W on level 7. On the induction cooktop, the broccoli was thus stir-fried for 2-3 min at 1500W, then 3-4 min at 750W.

After cooking for ~30 min, the pasta was drained by pouring the contents of the large pot into a colander over a bucket and then dumping the pasta back into the large pot. The plant-based meat sauce and broccoli were then added to the large pot with pasta and mixed. Following this, the technician covered the stockpot with pasta, the trash bin, and the bucket with water and left the room. This initiated a 30 min decay period.

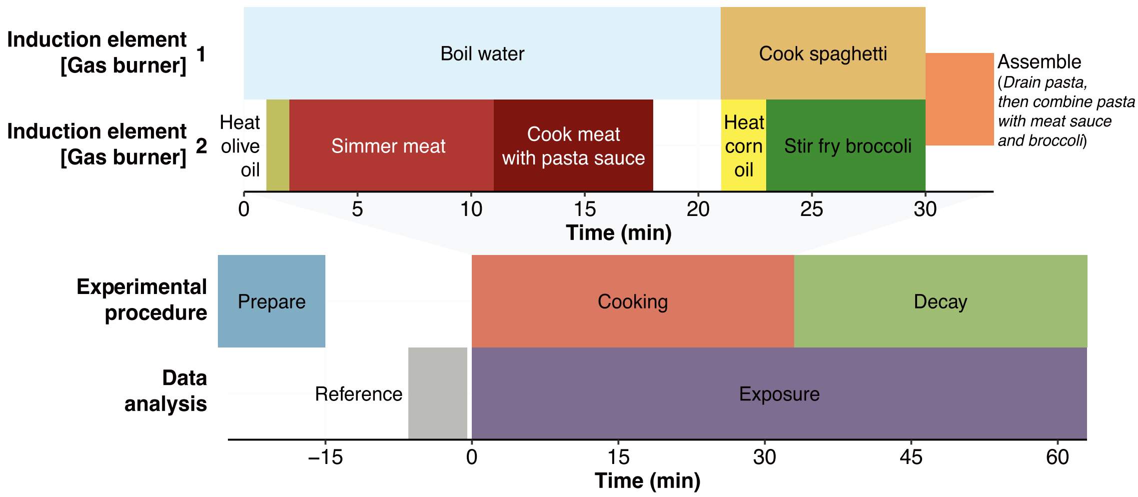

Figure 1. Cooking and experiment procedures. The top of the figure (a) summarizes the cooking procedures on each burner/element. The bottom section (b) shows the experimental sequence that includes preparations, cooking and post-cooking measurements.

Thermal conditions in the chamber were managed with a chilled slab and the forced air HVAC system. During experiments, the slab was maintained at ~20 °C. Prior to starting each experiment, the chamber was ventilated for 30-45 min at ~13 air changes per h (ACH) with outdoor air that was run through a minimum efficiency reporting value (MERV)16 filter. As needed, the system was then operated in a cooling mode with 100% recirculating air and maximum cooling capacity to reduce the room temperature to ~20 °C. The forced air heating and cooling (HVAC) system was turned off at least 10 min before cooking started to measure baseline pollutant concentrations. The HVAC system was kept off to prevent additional losses via ventilation and filtration during the cooking and decay period, and the air within the room was mixed with portable fans placed in three corners.

The entire sequence, including chamber air cleaning, food preparation, the cooking procedure, and post-cooking decay was repeated three times each for six scenarios: gas and induction cooktops were each used with no range hood operation, Hood A on or Hood B on.

Pollutant measurements

Pollutant concentrations were measured using a suite of monitors, as listed in Table 1. Instruments were located approximately in the center of the room. The sampling inlets were around 1.0–1.3 m above the chamber floor.

Table 1. List of Instrumentation used during cooking activities.

Analyte	Producer, model	Methods
Particle concentrations in 32 bins from 5.6 to 560 nm	TSI, 3091 Fast Mobility Particle Sizer (FMPS)	Electrical mobility with low-noise electrometers
Particle concentrations in 52 bins from 0.5 to 20 µm.	TSI, 3321 Aerodynamic Particle Sizer (APS)	Time-of-flight aerodynamic sizing with optical counter
Particle concentrations in 41 bins from 10 nm to 35 µm.	Grimm, Mini-Wide Range Aerosol Spectrometer (Mini-WRAS)	Combination of electrical mobility and optical particle detection
Particle concentrations in 16 bins from 0.5 to 10 µm.	TSI 3330 Optical Particle Sizer	Optical particle counter
NO_X, NO, and NO_2	Teledyne, API 200A	Chemiluminescence
Speciated VOCs	Ionicon, PTR-MS	Proton transfer reaction mass spectroscopy that tracks chemicals by mass to charge ratio (m/z)
O_3	2B Technologies, 205 Dual Beam Ozone Monitor	UV absorbance
CO_2	PP Systems, EGM-4	Non-dispersive infrared
Room air temperature / relative humidity	TSI, AirAssure	

Proton transfer reaction mass spectrometer

Proton transfer reaction mass spectrometry (PTR-MS) has been used as a valuable tool for indoor air quality research [30,31]. The principles of PTR-MS operation have been previously detailed [32,33]. In brief, PTR-MS measures VOCs with a proton affinity (PA) higher than that of water. It uses hydronium ions (H_3O^+) to ionize VOCs through proton transfer, resulting in ionized VOCs without fragmentation. These ions are then analyzed by their mass-to-charge ratio in a mass spectrometer, enabling continuous and sensitive detection of VOCs. During the measurement, the drift tube was operated at 2.2 mbar and 600 V, giving an E/N of~114 Td, which determines the drift velocity of the ions in the drift tube [32]. The PTR-MS was operated using the select ion mode, monitoring levels of 23 ions, for all experiments. As PTR-MS measures nominal masses of the product ions, we assigned tentative chemical structures for these ions, while noting the potential co-existence of isobaric compounds. Chemical concentrations were reported as counts per second (cps) and plotted with 1-minute average values for each ion.

Data analysis

For airborne particles, the mass concentration was estimated by first calculating the volume, assuming that all particles were spheres with diameters at the geometric mean value within each size bin, and then assuming a particle density of 1 $g \cdot cm^{-3}$ [34,35] For this calculation, we considered the FMPS and APS to be the primary suite of instruments, as the FMPS has a much lower particle size quantitation limit than the electrical mobility analyzer of the mini-WRAS, and the APS provides a more reliable size attribution based on aerodynamics. Mass concentration was also calculated using the combination of electrical mobility and OPC that is included in the Grimm mini-WRAS and with only the OPC sensor of the Grimm or the OPS. The latter two were used to explore the impact of trying to measure differences in emissions using only an optical instrument.

Using time-resolved monitoring data, we calculated the time-integrated concentrations of air pollutants as an indicator of the exposure that would occur during and following cooking in a home environment. The integration period included roughly 30 min of active cooking and an additional 30 min post-cooking. We use “exposure concentration”, denoted as $C_e(t)$, to represent the cooking-related pollutants in the chamber air at time t. It is calculated by subtracting the mean concentration during the reference period, $\overline{C_r}$, from the measured concentration, $C(t)$, as detailed in Eq. (1).

$$C_e(t) = C(t) - \overline{C_r} \tag{1}$$

The reference and exposure periods for each experiment can be found in Figures S2 and S3. We calculated the average exposure concentration over the hour, C_e, for scenario comparisons. Welch’s t-test (for two samples of uneven variance) was used to test the difference between each pair of conditions with three repeats. In addition, we applied a mixed-effects model to analyze the difference in exposure concentrations resulting from cooking the specified meal with the gas or induction cooktop under various range hood conditions, as detailed in Supporting Information 6. In this model, the cooktop was treated as the fixed effect, while the range hood served as the random effect. The statistical significance of differences in pollutant levels between the two types of cooktops was determined by the *p*-value from hypothesis testing. The null hypothesis asserted that cooktop type does not significantly affect pollutant concentrations. For both the Welch t-test and mixed effects models, the statistical discernibility/significance was reported at three levels: $p \geq 0.15$, labeled as "ns"; $0.05 \leq p < 0.15$, reported specific *p* values; and $p < 0.05$, marked as "< 0.05", the level that is most commonly used to indicate statistical significance.

To estimate the efficacy of each range hood on lowering pollutant exposure, we adopted crossed-factorial comparisons between the unpaired three replicates of baseline (hood off) and the three replicates of each intervention: Hood A or Hood B. We define *i* as the cooktop index ($i = 1$ for gas, $i = 2$ for induction), *j* as the range hood condition ($j = 0$ for No hood, $j = 1$ for Hood A, $j = 2$ for Hood B), and *k* as the index for the repeat measurement (1 to 3 repeats). The efficacy of range hood *j* with cooktop *i* under the *k*-th implementation of the range hood off and k'-th implementation of the intervention conditions can be written as:

$$EF_{i,j,k,k'} = \frac{\overline{C_e}(i, j = 0, k, k') - \overline{C_e}(i, j, k, k')}{\overline{C_e}(i, j = 0, k, k')} \times 100\% \qquad (2)$$

The mean efficacy is calculated as follows:

$$\overline{EF_{i,j}} = \frac{1}{9}\sum_{k=1}^{3}\sum_{k'=1}^{3} E_{i,j,k,k'} \qquad (3)$$

The standard deviation of the efficacy is given by:

$$\sigma_{E,i,j} = \sqrt{\frac{1}{8}\sum_{k=1}^{3}\sum_{k'=1}^{3}\left(EF_{i,j,k,k'} - \overline{EF_{i,j}}\right)^2} \qquad (4)$$

The same approach was used to calculate the difference in energy use between gas and induction cooktops.

RESULTS AND DISCUSSION

Food mass changes

Figure 2 summarizes the measurements of food mass consumed during three of the component cooking activities when using gas and induction cooktops. Cooking consumed around 22% of the mass of olive oil and plant-based meat, and about 18% of the mass of corn oil and broccoli. Stir-frying broccoli on the induction cooktop consumed slightly more mass than cooking on the gas burner (mean of 19.6% vs. 17.1%), with the difference marginally significant. The mass lost during the heating of the meat sauce was statistically significantly greater with induction cooking (mean of 7.6% vs. 6.8%); but less mass was lost during this activity relative to the other two. We did not measure the increase in pasta mass or the reduction in mass of the water used to cook the pasta.

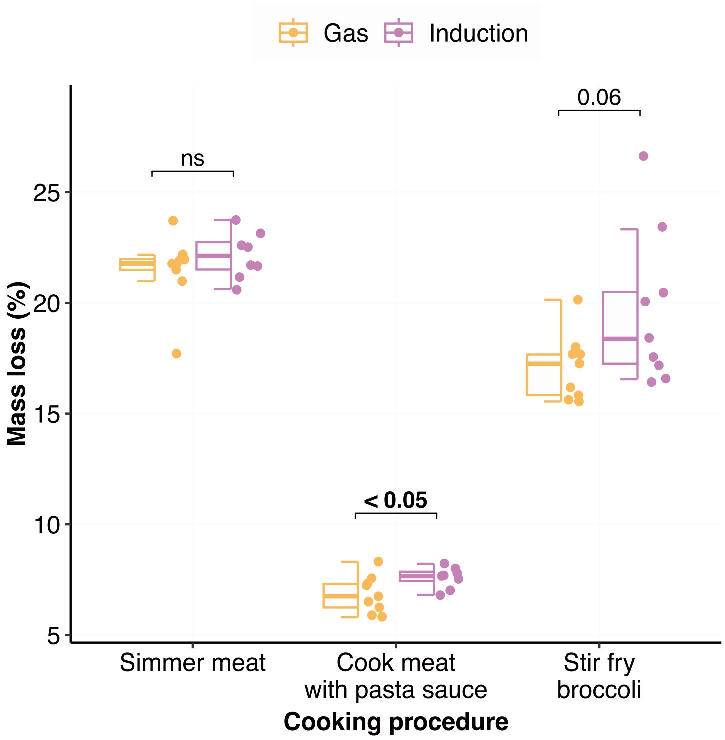

Figure 2. Changes in food mass during different cooking procedures when using gas and induction elements. Comparisons show p-values calculated with Welch's t-test; "ns" indicates a non-significant difference, with *p*-value >0.15.

Changes in thermal environments

As shown in Figure 3, cooking with gas or induction cooktops raised the room air temperature and relative humidity by 2.5 °C and 2% respectively, with no statistically significant difference between the two. Consistent with water vapor production during combustion, the gas cooking raised the absolute humidity more than cooking with induction. It is important here to note that water vapor was released from the heating of food with both cooktops.

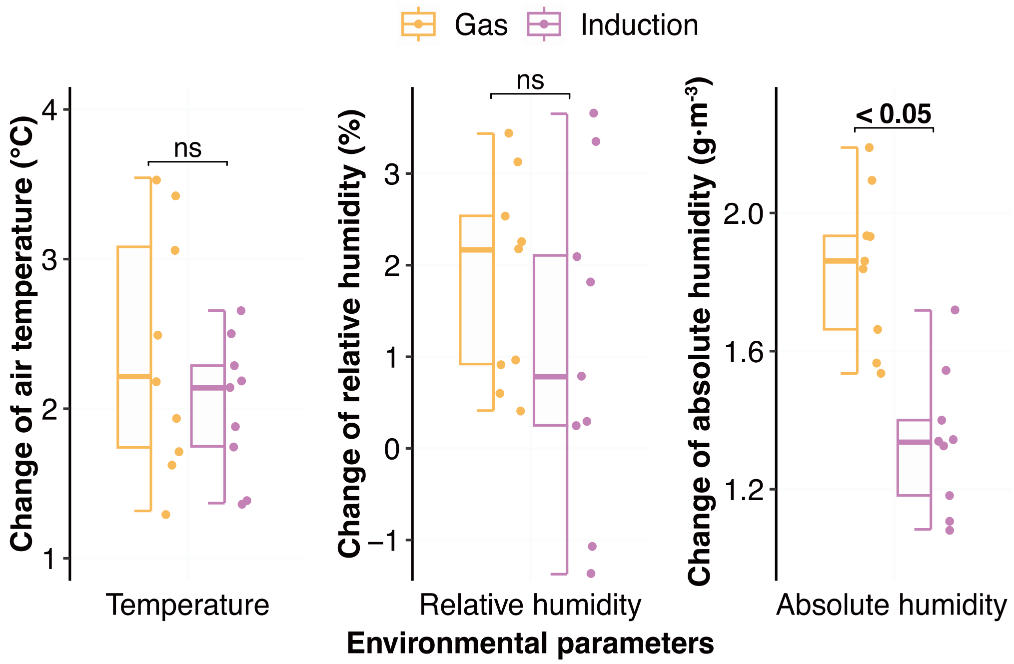

Figure 3. Average changes in temperature, relative humidity, and absolute humidity relative to the reference period for each test. Comparisons show p-values calculated with Welch's t-test; "ns" indicates a non-significant difference, with *p*-value >0.15.

Energy consumption of cooktops

Figure 4 shows the time-resolved power and total energy input to the gas and induction cooktops during all studied conditions. The power use profiles reflect consistent application of the cooking procedures across experiments and conditions, with just minor variations. The non-steady sequence of power input during the cooking of broccoli was necessitated by the goal of matching the total energy delivered to the food when cooking on the different cooktops, as described in the Methods.

Overall energy consumed was twice as high on the gas burners as it was on the induction cooktop, reflecting the higher efficiency of induction cooking technology. For the gas burners only, total energy use was marginally higher (with statistical significance of $p<0.05$) when the range hoods were operating compared to experiments without range hood use. The condition of the gas cooktop without a range hood operating includes only two experiments since the methane flow measurement stopped logging early on one experiment.

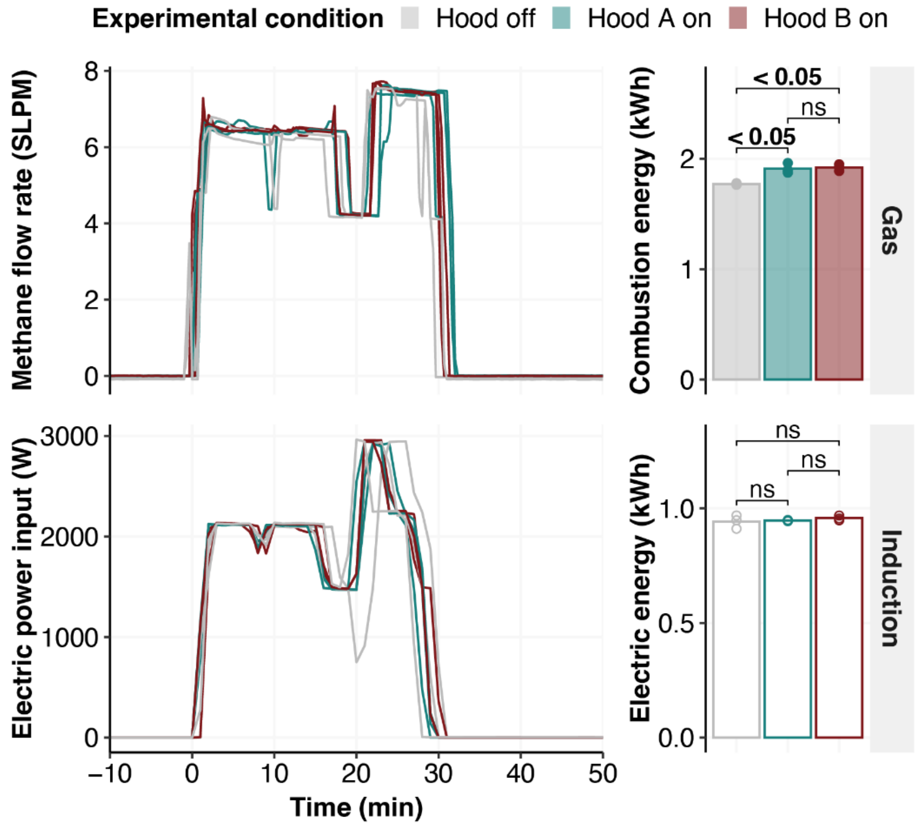

Figure 4. Time-resolved methane energy flow to the gas cooktop and electric power input for the induction cooktop, and the respective total energy consumptions. Power and energy for the gas cooktop were calculated using the lower heating value of methane of 50 $KJ \cdot g^{-1}$. Comparisons show p-values calculated with Welch's t-test; "ns" indicates a non-significant difference, with *p*-value >0.15.

Inorganic gas pollutants

Figure 5 presents the time-resolved exposure concentrations of NO_X, NO, NO_2, and CO_2. When using the gas cooktop, the concentration of these compounds increased from the start to the end of cooking and did so consistently across experiments. By the end of cooking, the concentrations of NO_x and CO_2 rose, on average, to around 440 ppb and 1000 ppm above the baseline levels before cooking. This is consistent with the well-documented process of NO_X forming from reactions of nitrogen and oxygen in the high-temperature regions of flames and the production of CO_2 during combustion. When using the induction cooktop, there was no discernible increase of NO_x, NO, or NO_2 and CO_2 increased by less than 100 ppm. For both cooktops, respiration of the 1-2 research staff conducting the experiments contributed to the observed CO_2. The O_3 concentration decreased after the start of cooking (Figure S5), and no difference was found among conditions.

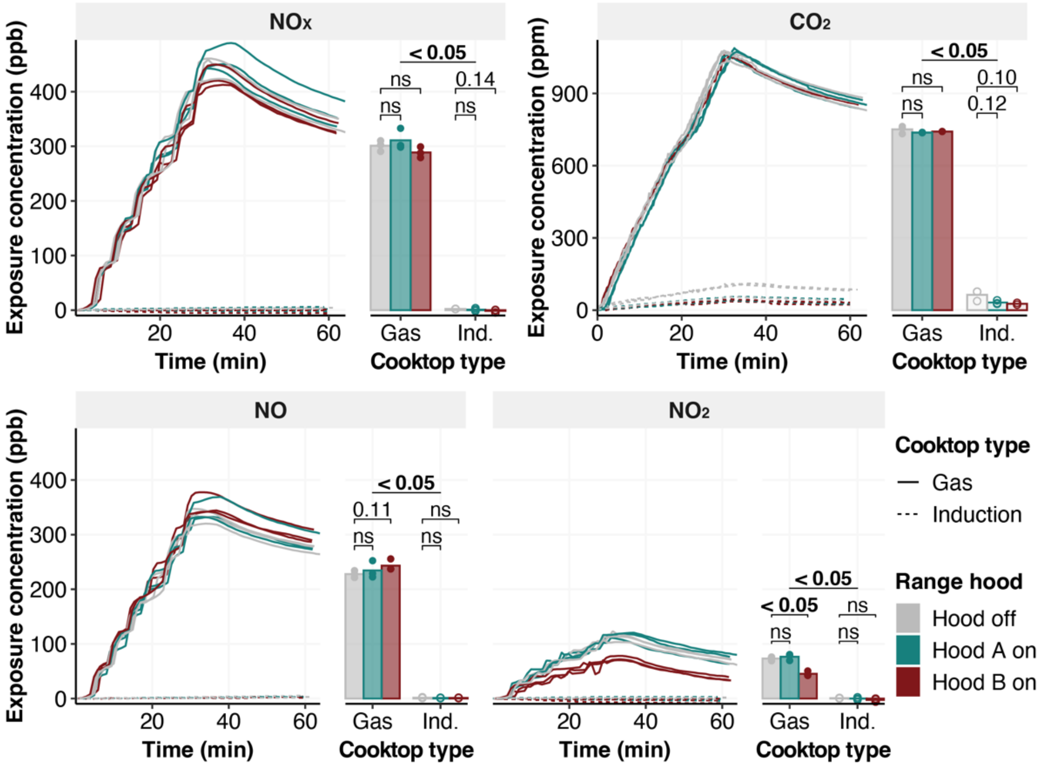

Figure 5. Time-resolved and averaged exposure concentrations of NO_X, NO, NO_2, and CO_2 during gas and induction cooking under three range hood conditions. Each solid or hollow point represents the average net exposure concentration during the exposure period of each experiment.

Using the recirculating range hoods generally didn't impact the inorganic gas concentrations in the room. The exception is that using Hood B substantially and significantly lowered the NO_2 concentration and resulted in a small and marginally significant (p=0.11) increase in NO.

Airborne particles

Figure 6 illustrates the time-resolved and event-averaged exposure concentrations of UFPs, $PM_{2.5}$, and PM_{10} resulting from gas and induction cooking, based on data from the FMPS and APS instruments. While cooking with both fuels generated particles that varied in size from sub- to super-micron and included substantial mass in the $PM_{2.5}$ and coarse (diameters between 2.5 and 10 microns) modes, the biggest difference was the much larger production of UFPs when cooking with gas. As with NO_X, the difference in UFPs between cooking with gas vs. induction cooktops results from the lack of combustion and thus lack of substantial UFP formation by the induction element; UFPs are generated through incomplete combustion and chemical reactions in the high-temperature flame environment. The top left panel of Figure 6 shows that UFPs were emitted from the gas burner during all phases of cooking, whereas cooking with induction produced relatively few UFPs. In contrast to inorganic pollutants that accumulated steadily during gas cooking, increases in particle concentrations varied by size fraction and during the different cooking procedures. Peak concentrations of UFPs and most of the $PM_{2.5}$, and PM_{10} produced during the meal were associated with stir-frying the broccoli. As summarized in Table S2, when cooking with gas and the hood off, the average (and standard deviation among repeats) exposure concentrations of UFPs, $PM_{2.5}$, and PM_{10} were

38.5 (1.5) × 10^4 #·cm^{-3}, 13.2 (4.7) μg·m^{-3}, and 20.3 (8.6) μg·m^{-3}, with peaks reaching 104.3 (11.3) × 10^4 #·cm^{-3}, 29.7 (12.3) μg·m^{-3}, and 61.7 (30.4) μg·m^{-3}. With no hood use, exposure concentrations of UFPs were nearly two orders of magnitude higher when using the gas cooktop compared to the induction cooktop. Based on particle counts from the FMPS and APS, cooking with induction produced higher $PM_{2.5}$ and PM_{10} concentrations relative to cooking with gas—increases of 62% and 132%, respectively, based on the mixed-effect model reported in Table S2, with the difference marginally statistically significant for $PM_{2.5}$ and significant for PM_{10}.

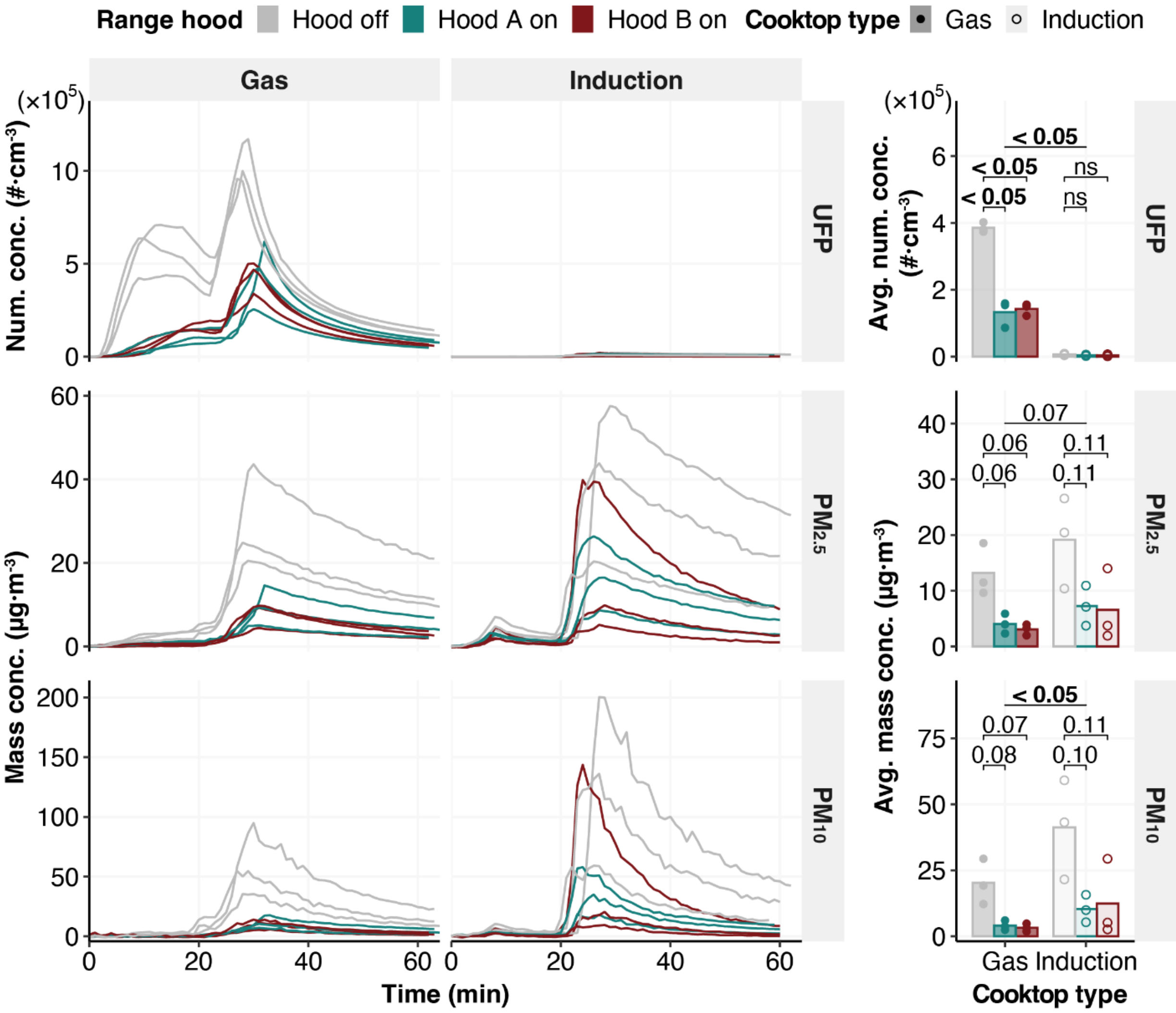

Figure 6. Time-resolved (left) and time-averaged (columns at right) exposure concentrations of UFPs, $PM_{2.5}$, and PM_{10} during gas and induction cooking under three range hood conditions. Each solid or hollow point represents the average net exposure concentration during the exposure period of each experiment.

UFP number concentrations and $PM_{2.5}$ and PM_{10} mass concentrations were also calculated using the size-resolved measurements of the Grimm Mini-WRAS (Figure S6). The electrical mobility analyzer of the Mini-WRAS has a higher minimum particle size than the FMPS and it reported a slightly different size distribution, as shown in Figures S7 and S8. The attributed size differences resulted in higher estimates of $PM_{2.5}$ for the gas burners based on the Mini-WRAS than calculations based on the FMPS and APS. $PM_{2.5}$ calculated from the size-resolved measurements of the Grimm were not discernibly higher for induction vs. gas; but a difference in PM_{10} remained discernible.

To the extent that the cooktop fuel impacted PM emissions, we hypothesize that it may have been caused by hotter pan surfaces when the induction elements were set to the higher power setting during the first part of the broccoli stir-fry or from more spatially varied pan surface temperatures leading to some hotter pan sites. While our team members who conducted the cooking observed no differences in the appearance or texture of the broccoli cooked with induction versus gas burners, the difference in mass consumed suggests a small difference in cooking that could account for the higher $PM_{2.5}$ and PM_{10}.

Figure 7 presents the calculated mass proportions of $PM_{0.1}$ (the calculated mass of UFPs), $PM_{0.1–0.3}$, and $PM_{0.3–2.5}$ within $PM_{2.5}$, again using the particle counts of the FMPS+APS. The size ranges were selected to assess how much the UFP contributed to $PM_{2.5}$ and how much of the mass of $PM_{2.5}$ was in particle sizes that are not quantitatively measured by devices that utilize light scattering [35–39]. These include optical particle counters, photometers, and integrating nephelometers. When cooking with gas and the range hood off, the $PM_{0.1}$ fraction rose similarly to UFP (Figure 6), stabilizing at approximately 45% after the meat sauce was completed. Particles smaller than 0.3 um accounted for about 50% of the $PM_{2.5}$. When using a recirculating range hood with filters, the $PM_{0.1}$ proportion was lower; but the proportion of $PM_{0.1–0.3}$ increased, resulting in a similar mass fraction of $PM_{2.5}$ in particles with diameters <0.3 µm. These results indicate that roughly half of the $PM_{2.5}$ emitted when using gas burners to cook the meal prepared in this experiment would not be fully quantified by an OPC or other optical device. In contrast, $PM_{0.1}$ and $PM_{0.1–0.3}$ proportions in $PM_{2.5}$ were less than 5% and 8% when using the induction cooktop with the hood off. In Figure S9, we further compared the $PM_{2.5}$ concentrations calculated based on size-resolved OPC to those by FMPS+APS and Mini-WRAS. The OPS underestimated the $PM_{2.5}$ concentrations during the gas cooking due to the limitation of the lower detection limit of 0.3 µm. However, OPS tended to report higher $PM_{2.5}$ concentrations during induction cooking due to a higher number concentration between 1 and 2.5 µm (Figures S7 and S8). These differences underscore how the particle size distribution can influence the accuracy of optical particle sensors in measuring mass concentrations and also that reliance solely on an optical sensor to evaluate potential differences in emissions between cooktop technologies can lead to a biased result.

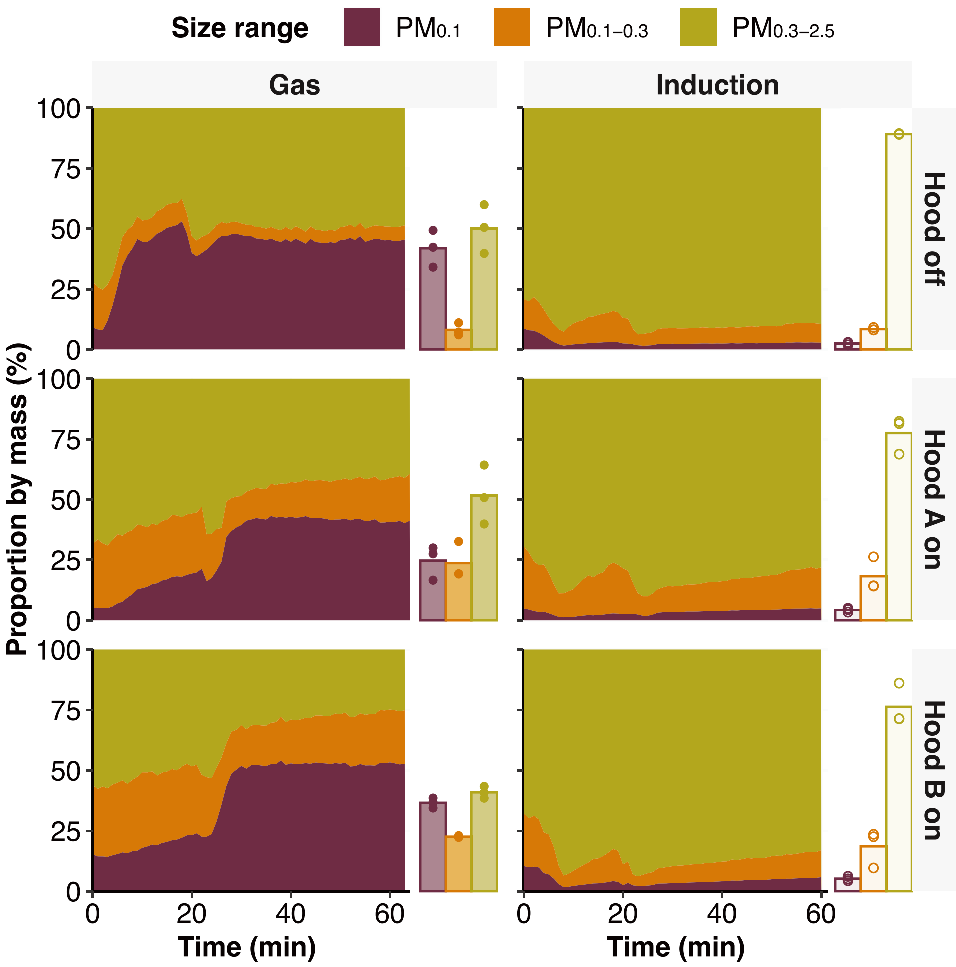

Figure 7. The time-resolved mass proportion of $PM_{0.1}$, $PM_{0.1-0.3}$, and $PM_{0.3-2.5}$ within $PM_{2.5}$ for a single experiment conducted with each combination of cooktop (gas, induction) and range hood (No hood, Hood A, Hood B). In the column charts, dots represent the average proportions from each test, while bars indicate the overall average of the three repeats.

Volatile organic compounds

Figure 8 shows the time-resolved exposure concentrations of all sixteen VOCs across sixteen tests. For most compounds, including ethanol, acrolein, acetone, isoprene, limonene, benzene, ethylbenzene, and toluene, concentrations increased throughout the cooking process, without clear impacts from the specific cooking activities. And their rising concentrations correspond temporarily with an increase in both temperature and humidity in the room (Figure S4). It is therefore possible that some of the observed increase in these VOCs could be from a change in the partitioning of previously adsorbed chemicals with increasing temperature. In contrast, concentrations of methanol, butanal, acetic acid, and ethyl acetate rose noticeably during the meat simmering. Stir-frying of broccoli led to sharp increases in methanol, methanethiol, and dimethyl sulfide. During the 30 min decay period, after cooking finished, concentrations of most of the compounds started to decrease while those of toluene and ethylbenzene continued to increase in no hood and Hood A experiments.

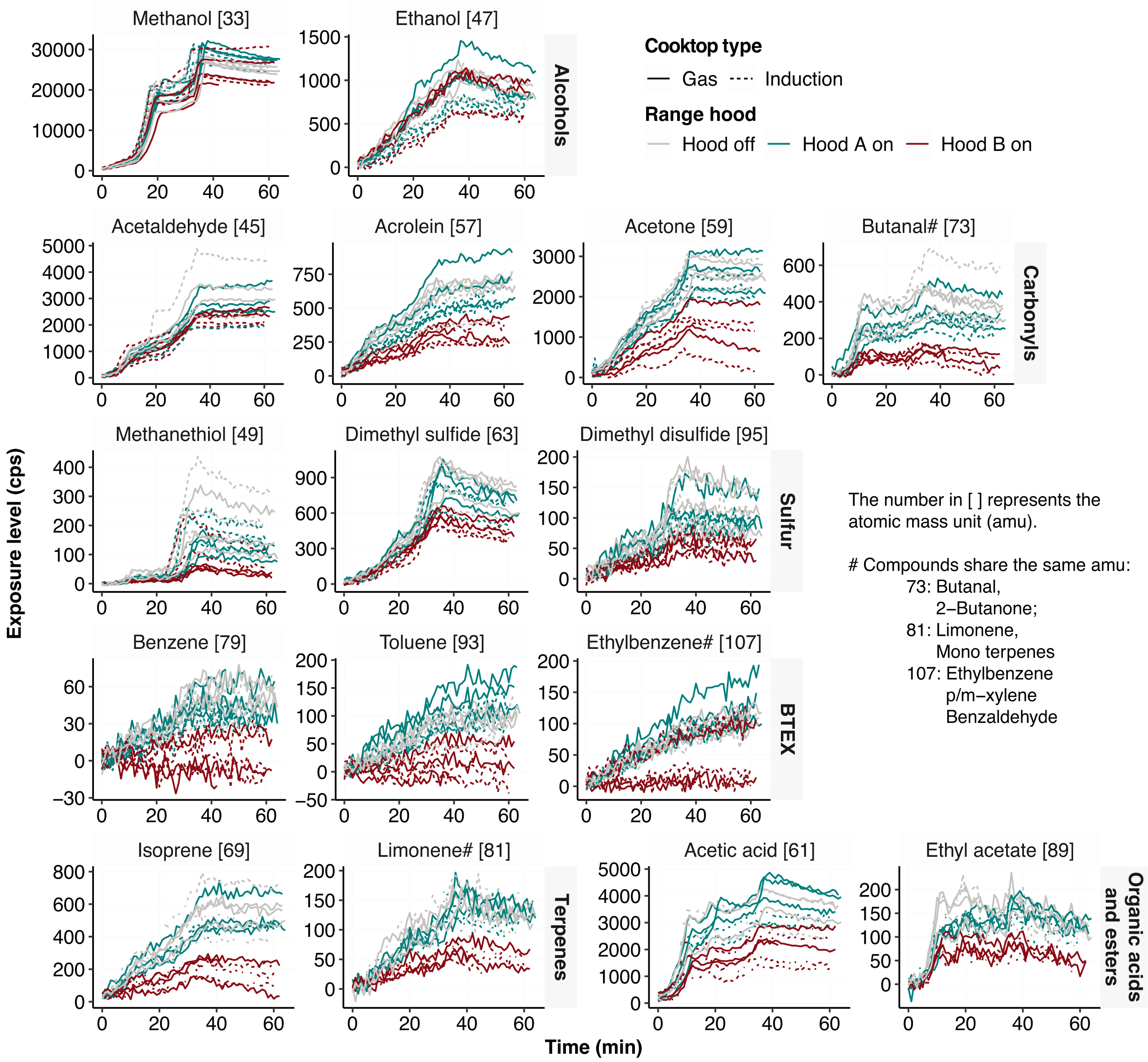

Figure 8. Time-resolved concentrations of VOCs using gas and induction cooktops under three range hood conditions.

Figure 9 summarizes the average exposure concentrations of each VOC throughout the cooking and decay periods. Through mixed-effect modeling, we identified that the concentrations of ethanol, acetic acid, dimethyl sulfide, toluene, and acrolein were significantly or weakly significantly lower when cooking with an induction cooktop compared to a gas cooktop. Conversely, methanethiol concentrations were found to be weakly significantly higher when cooking with the induction cooktop. The impact of the two range hoods on VOC concentrations varied. Hood A exhibited no significant impact whereas Hood B effectively reduced exposure levels for the majority of the measured VOCs.

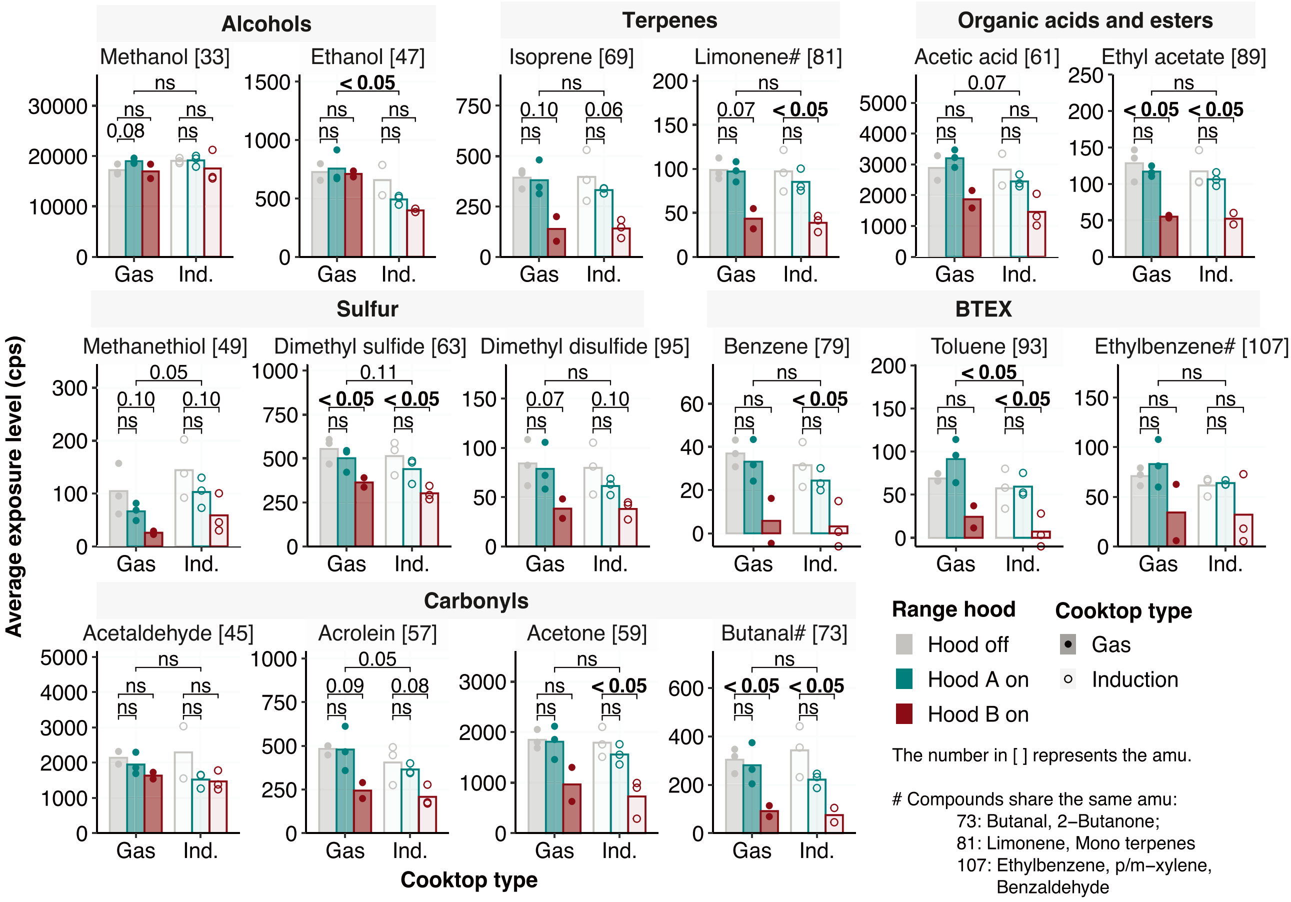

Figure 9. Average exposure concentration of VOCs using gas and induction cooktops under three range hood conditions.

Calculated efficacies of the recirculating range hoods with filters

Figure 10 illustrates the effectiveness of the two recirculating range hoods used in our experiments in reducing exposure to airborne particles and VOCs for the studied meal. For airborne particles, both range hoods demonstrated comparable efficacy, reducing exposure by 40% to 80% across particle size fractions, with a noted increase in effectiveness for larger particle sizes. The reduction in exposure was greater when cooking with the gas cooktop compared to the induction cooktop across all three particle size ranges. This difference is presumably related to the different distributions of particle mass by size that resulted from cooking using gas or induction.

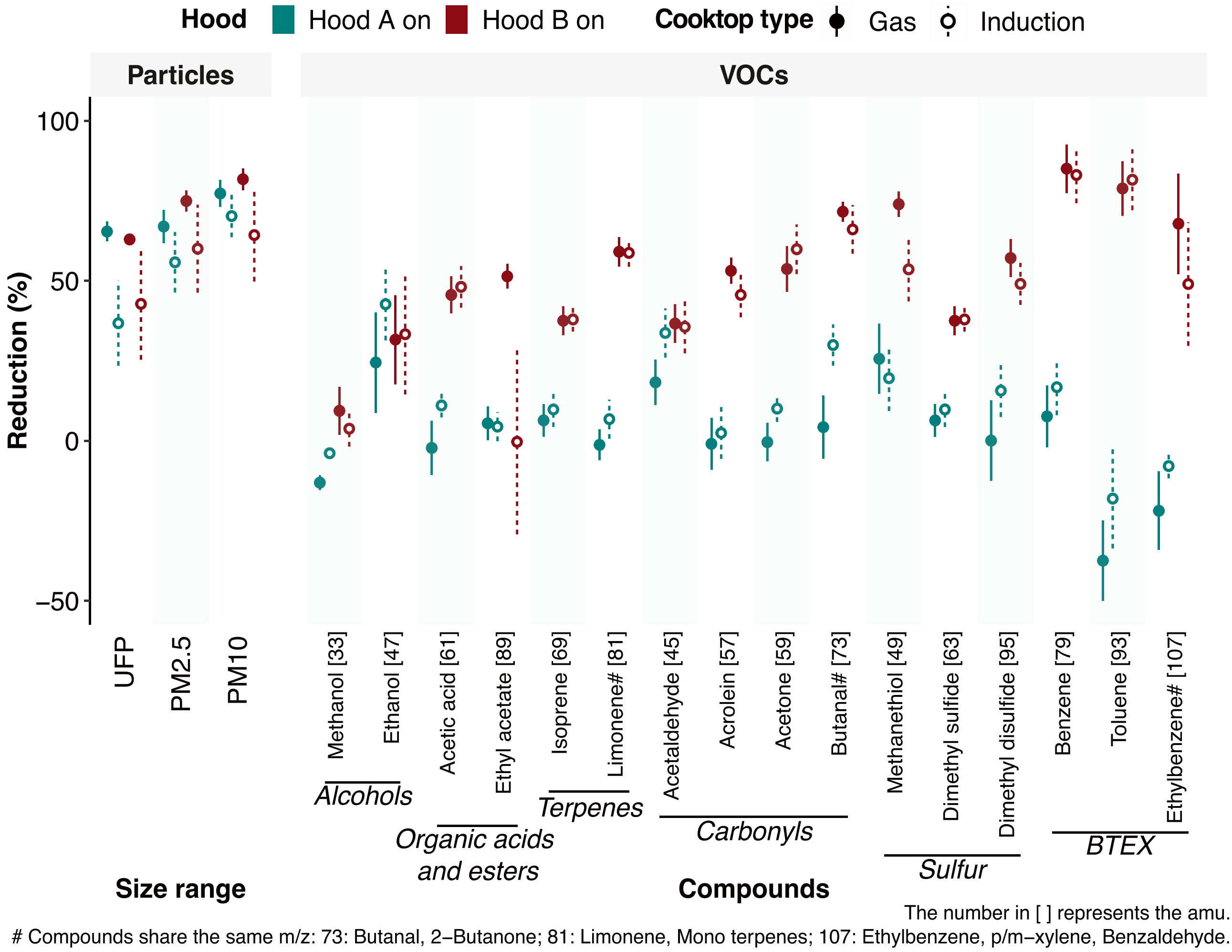

Figure 10. The reduction of airborne particles and VOCs by using the two range hoods.

In contrast to the comparable performance in particle reduction, the two range hoods had very different impacts on VOC exposure concentrations. Range Hood B reduced exposure concentrations for most VOCs, particularly for BTEX (Benzene, Toluene, Ethylbenzene, and Xylenes), which saw the most significant decreases. The reductions in exposure to alcohol compounds were the least pronounced.

Strengths, limitations, and future research

Study strengths include the use of a large room that is similar in size to many "great rooms" or areas in homes that include the kitchen, thus resulting in concentration ranges that are broadly representative of cooking in homes [40–42]. Working at representative concentrations means that the gas-particle dynamics are also likely to be representative. The food preparation was realistic and included actions of the cook, rather than an idealized procedure that excluded the cook. The cooking procedures were carefully documented and repeated multiple times. The meal also included three different common cooking activities.

The key limitation in comparing gas to induction was the testing of only one meal. Given that this pilot study examined only a single meal, the finding that cooking with the induction cooktop yielded higher $PM_{2.5}$ (on one of two sets of instruments) and higher PM_{10} (on both) should not be considered necessarily generalizable to all cooking. By contrast, the finding of almost no NO_X and very low UFP when cooking with induction should be considered as very robust. The variability of emissions associated with cooking and the modest replicability of three experiments for each condition limited our ability to discern statistically significant differences for some pollutants. This study was also limited in the number of recirculating range hoods that were studied (two), and did not include any in-depth exploration of the fundamental physical-chemical processes that underlie the observed results. Specifically, it would be fruitful to try to discern the contributions of Hood A's grease impactor and Hood B's grease screen to PM reduction.

The results of this study demonstrate the potential value of more research to quantify emissions from cooking of other dishes and more varied cooking with gas and induction. It is also worthwhile to examine other recirculating range hoods with air cleaning technologies. It would be beneficial for these studies to include more replicates to increase statistical power and to delve into the physical mechanisms of pollutant generation and removal that produce the observable, bulk effects, e.g., using thermographic imaging to identify potential differences in cooking temperatures.

CONCLUSIONS

This study successfully demonstrated an approach for comparing the pollutant exposure impacts of cooking with gas versus induction cooktops by carefully repeating the preparation of a meal consisting of pasta, a plant-based meat sauce, and stir-fried broccoli in a 158 m^3 room.

Time-resolved measurements during cooking and 30 min following cooking showed that emissions of nitrogen oxides (and nitrogen dioxide) were effectively eliminated and ultrafine particles were greatly reduced when cooking with induction, compared to gas burners. $PM_{2.5}$ estimated from measurements of size-resolved particle number concentrations was likely higher for cooking the specified meal with induction compared to gas; but the statistical discernibility varied based on the particle instrumentation. Estimated PM_{10} exposure concentrations were discernibly higher with particle counts from all of the instruments used. There were small differences in concentrations of some volatile organic compounds but no overall trends across the 30 VOCs measured.

About half of the $PM_{2.5}$ resulting from cooking with gas was in particles that were smaller than 0.3 µm, which is the lower quantitation threshold for many optical particle instruments. The fraction of $PM_{2.5}$ in this size range is much lower when cooking with induction. The implication of this is that use of optically-based particle monitors to evaluate the effect of cooking fuel on PM emissions would provide biased results for the specific meal that was studied, and the bias could also occur with other meals.

Both of the recirculating range hoods with filters that were tested in this study substantially reduced all particle sizes when cooking with gas or induction, with larger reductions for gas cooking. One of the range hoods also substantially lowered some of the VOCs.

Funding

This work was supported by the Building America Program within the Building Technologies Office of the U.S. Department of Energy under Contract No. DE-AC02-05CH11231. Additional support was provided by the U.S. Environmental Protection Agency Indoor Environments Division under Interagency Agreement DW 089 92572701. The two tested range hoods and air filters were provided by Fotile and Miele from normal supply chain stock.

Acknowledgements

We thank the FLEXLAB team (Hershow Al-Barazi, Matthew McCloskey, William Holland, Stacy Curry, and Cynthia Regnier) for their expert technical assistance, flexibility and patience, without which this project could not have been done. Stein Shi and Steve Polinski helped with the identification of recirculating range hoods that met the selection criteria and arranged for one of each to be provided. Jerry Zhang and Marco Weichart provided information about the air cleaning technologies featured in the two range hoods. We thank Kyle Biega and Amy Royden-Bloom for helpful comments about the draft manuscript.

REFERENCES

[1] J.D. Spengler, M. Brauer, J.M. Samet, W.E. Lambert, Nitrous-Acid in Albuquerque, New-Mexico, Homes, Environ. Sci. Technol. 27 (1993) 841–845. https://doi.org/DOI 10.1021/es00042a005.

[2] C.W. Spicer, D.V. Kenny, G.F. Ward, I.H. Billick, Transformations, lifetimes, and sources of NO2, HONO, and HNO3 in indoor environments, Air Waste 43 (1993) 1479–1485.

[3] M. Dennekamp, S. Howarth, C.A.J. Dick, J.W. Cherrie, K. Donaldson, A. Seaton, Ultrafine particles and nitrogen oxides generated by gas and electric cooking, Occup. Environ. Med. 58 (2001) 511–516. https://doi.org/10.1136/oem.58.8.511.

[4] K. Lee, X.P. Xue, A.S. Geyh, H. Ozkaynak, B.P. Leaderer, C.J. Weschler, J.D. Spengler, Nitrous acid, nitrogen dioxide, and ozone concentrations in residential environments, Environ. Health Perspect. 110 (2002) 145–149.

[5] N.A. Mullen, J. Li, M.L. Russell, M. Spears, B.D. Less, B.C. Singer, Results of the California Healthy Homes Indoor Air Quality Study of 2011-2013: impact of natural gas appliances on air pollutant concentrations, Indoor Air 26 (2016) 231–45. https://doi.org/10.1111/ina.12190.

[6] B.C. Singer, R.Z. Pass, W.W. Delp, D.M. Lorenzetti, R.L. Maddalena, Pollutant concentrations and emission rates from natural gas cooking burners without and with range hood exhaust in nine California homes, Build. Environ. 122 (2017) 215–229. https://doi.org/10.1016/j.buildenv.2017.06.021.

[7] E.D. Lebel, C.J. Finnegan, Z. Ouyang, R.B. Jackson, Methane and NOx Emissions from Natural Gas Stoves, Cooktops, and Ovens in Residential Homes, Environ. Sci. Technol. 56 (2022) 2529–2539. https://doi.org/10.1021/acs.est.1c04707.

[8] P. Jacobs, D. Moretti, A. Beelen, E. Cornelissen, E. Topal, O. Vijlbrief, L. Hoes, Health effects in EU from cooking on gas: phase II field study, 2023. https://publications.tno.nl/publication/34641471/zD0Xiz/TNO-2023-R11809.pdf.

[9] S. Patel, S. Sankhyan, E.K. Boedicker, P.F. DeCarlo, D.K. Farmer, A.H. Goldstein, E.F. Katz, W.W. Nazaroff, Y. Tian, J. Vanhanen, M.E. Vance, Indoor Particulate Matter during

HOMEChem: Concentrations, Size Distributions, and Exposures, Environ. Sci. Technol. 54 (2020) 7107–7116. https://doi.org/10.1021/acs.est.0c00740.

[10] B. Less, N. Mullen, B. Singer, I. Walker, Indoor air quality in 24 California residences designed as high-performance homes, Sci. Technol. Built Environ. 21 (2015) 14–24. https://doi.org/10.1080/10789669.2014.961850.

[11] L. Wallace, F. Wang, C. Howard-Reed, A. Persily, Contribution of gas and electric stoves to residential ultrafine particle concentrations between 2 and 64 nm: size distributions and emission and coagulation remission and coagulation rates, Environ. Sci. Technol. 42 (2008) 8641–7.

[12] L.A. Wallace, W.R. Ott, C.J. Weschler, Ultrafine particles from electric appliances and cooking pans: experiments suggesting desorption/nucleation of sorbed organics as the primary source, Indoor Air 25 (2015) 536–546. https://doi.org/10.1111/ina.12163.

[13] K.L. Abdullahi, J.M. Delgado-Saborit, R.M. Harrison, Emissions and indoor concentrations of particulate matter and its specific chemical components from cooking: A review, Atmos. Environ. 71 (2013) 260–294. https://doi.org/10.1016/j.atmosenv.2013.01.061.

[14] L. Sun, L.A. Wallace, Residential cooking and use of kitchen ventilation: The impact on exposure, J. Air Waste Manag. Assoc. 71 (2021) 830–843. https://doi.org/10.1080/10962247.2020.1823525.

[15] Q.F. Zhang, R.H. Gangupomu, D. Ramirez, Y.F. Zhu, Measurement of ultrafine particles and other air pollutants emitted by cooking activities, Int. J. Environ. Res. Public. Health 7 (2010) 1744–1759. https://doi.org/10.3390/ijerph7041744.

[16] D.A. Olson, J.M. Burke, Distributions of PM2.5 source strengths for cooking from the research triangle park particulate matter panel study, Environ. Sci. Technol. 40 (2006) 163–169. https://doi.org/10.1021/es050359t.

[17] G. Buonanno, L. Morawska, L. Stabile, Particle emission factors during cooking activities, Atmos. Environ. 43 (2009) 3235–3242. https://doi.org/10.1016/j.atmosenv.2009.03.044.

[18] M. Amouei Torkmahalleh, S. Gorjinezhad, H.S. Unluevcek, P.K. Hopke, Review of factors impacting emission/concentration of cooking generated particulate matter, Sci. Total Environ. 586 (2017) 1046–1056. https://doi.org/10.1016/j.scitotenv.2017.02.088.

[19] F. Johnson, R. Swierczyna, B. Sutherland, J. Fixier, Cooking Emissions from Food for Natural Gas, Propane and Electric Range Tops, ASHRAE Trans. 130 (2024) 161–166.

[20] M. Daouda, A. Carforo, H. Miller, J. Ventrella, Y.A. Tan, M. Feliciano, J. Tryner, A. Hallward-Driemeier, S. Chillrud, R. Commane, D. Hernández, M. Johnson, D. Jack, Out of Gas, In with Justice: Findings from a gas-to-induction pilot in low-income housing in NYC, Energy Res. Soc. Sci. 116 (2024) 103662. https://doi.org/10.1016/j.erss.2024.103662.

[21] W.W. Delp, B.C. Singer, Performance assessment of U.S. residential cooking exhaust hoods, Environ. Sci. Technol. 46 (2012) 6167–6173. https://doi.org/10.1021/es3001079.

[22] S.M. Holm, J. Balmes, D. Gillette, K. Hartin, E. Seto, D. Lindeman, D. Polanco, E. Fong, Cooking behaviors are related to household particulate matter exposure in children with asthma in the urban East Bay Area of Northern California, PLOS ONE 13 (2018) e0197199. https://doi.org/10.1371/journal.pone.0197199.

[23] M.M. Lunden, W.W. Delp, B.C. Singer, Capture efficiency of cooking-related fine and ultrafine particles by residential exhaust hoods, Indoor Air 25 (2015) 45–58. https://doi.org/10.1111/ina.12118.

[24] C. O'Leary, Y. Kluizenaar, P. Jacobs, W. Borsboom, I. Hall, B. Jones, Investigating measurements of fine particle ($PM_{2.5}$) emissions from the cooking of meals and mitigating exposure using a cooker hood, Indoor Air 29 (2019) 423–438. https://doi.org/10.1111/ina.12542.

[25] L. Sun, L.A. Wallace, N.A. Dobbin, H. You, R. Kulka, T. Shin, M. St-Jean, D. Aubin, B.C. Singer, Effect of venting range hood flow rate on size-resolved ultrafine particle concentrations from gas stove cooking, Aerosol Sci. Technol. 52 (2018) 1370–1381. https://doi.org/10.1080/02786826.2018.1524572.

[26] X. Xu, K. Hu, Y. Zhang, J. Dong, C. Meng, S. Ma, Z. Liu, Experimental evaluation of the impact of ventilation on cooking-generated fine particulate matter in a Chinese apartment kitchen and adjacent room, Environ. Pollut. 348 (2024) 123821. https://doi.org/10.1016/j.envpol.2024.123821.

[27] L. Sun, B.C. Singer, Cooking methods and kitchen ventilation availability, usage, perceived performance and potential in Canadian homes, J. Expo. Sci. Environ. Epidemiol. 33 (2023) 439–447. https://doi.org/10.1038/s41370-023-00543-z.

[28] P. Jacobs, E. Cornelissen, Efficiency of recirculation hoods with regard to PM2.5 and NO2, in: Lublin, Poland, 2017.

[29] W. Wojnowski, A. Yang, T. Mikoviny, A. Wisthaler, K. Thunshelle, Exposure to cooking emitted volatile organic compounds with recirculating and extracting ventilation solutions, Build. Environ. 261 (2024) 111743. https://doi.org/10.1016/j.buildenv.2024.111743.

[30] S. Liu, R. Li, R.J. Wild, C. Warneke, J.A. de Gouw, S.S. Brown, S.L. Miller, J.C. Luongo, J.L. Jimenez, P.J. Ziemann, Contribution of human-related sources to indoor volatile organic compounds in a university classroom, Indoor Air 26 (2016) 925–938. https://doi.org/10.1111/ina.12272.

[31] T. Schripp, S. Etienne, C. Fauck, F. Fuhrmann, L. Märk, T. Salthammer, Application of proton-transfer-reaction-mass-spectrometry for Indoor Air Quality research, Indoor Air 24 (2014) 178–189. https://doi.org/10.1111/ina.12061.

[32] J. de Gouw, C. Warneke, Measurements of volatile organic compounds in the earth's atmosphere using proton-transfer-reaction mass spectrometry, Mass Spectrom. Rev. 26 (2007) 223–257. https://doi.org/10.1002/mas.20119.

[33] W. Lindinger, A. Jordan, Proton-transfer-reaction mass spectrometry (PTR–MS): on-line monitoring of volatile organic compounds at pptv levels, Chem. Soc. Rev. 27 (1998) 347–375. https://doi.org/10.1039/A827347Z.

[34] B.C. Singer, W.W. Delp, Response of consumer and research grade indoor air quality monitors to residential sources of fine particles, Indoor Air 28 (2018) 624–639. https://doi.org/10.1111/ina.12463.

[35] Z. Wang, W.W. Delp, B.C. Singer, Performance of low-cost indoor air quality monitors for PM2.5 and PM10 from residential sources, Build. Environ. 171 (2020) 106654. https://doi.org/10.1016/j.buildenv.2020.106654.

[36] J. Burkart, G. Steiner, G. Reischl, H. Moshammer, M. Neuberger, R. Hitzenberger, Characterizing the performance of two optical particle counters (Grimm OPC1.108 and OPC1.109) under urban aerosol conditions, J. Aerosol Sci. 41 (2010) 953–962. https://doi.org/10.1016/j.jaerosci.2010.07.007.

[37] C.M. Sorensen, J. Gebhart, T.J. O'Hern, D.J. Rader, Optical Measurement Techniques: Fundamentals and Applications, in: Aerosol Meas., John Wiley & Sons, Ltd, 2011: pp. 269–312. https://doi.org/10.1002/9781118001684.ch13.

[38] W.W. Szymanski, A. Nagy, A. Czitrovszky, Optical particle spectrometry—Problems and prospects, J. Quant. Spectrosc. Radiat. Transf. 110 (2009) 918–929. https://doi.org/10.1016/j.jqsrt.2009.02.024.

[39] R. Xu, Light scattering: A review of particle characterization applications, Particuology 18 (2015) 11–21. https://doi.org/10.1016/j.partic.2014.05.002.

[40] R. Fortmann, P. Kariher, R. Clayton, Indoor air quality: Residential cooking exposures, Prepared for California Air Resources Board, Sacramento, CA, 2001.

[41] C. He, Contribution from indoor sources to particle number and mass concentrations in residential houses, Atmos. Environ. 38 (2004) 3405–3415. https://doi.org/10.1016/j.atmosenv.2004.03.027.

[42] C.M. Long, H.H. Suh, P. Koutrakis, Characterization of Indoor Particle Sources Using Continuous Mass and Size Monitors, J. Air Waste Manag. Assoc. 50 (2000) 1236–1250. https://doi.org/10.1080/10473289.2000.10464154.

SUPPORTING INFORMATION

1 The cooking area

A cooking area was set up against an outside wall, as shown in Figure S1. A metal strut structure was used to mount the cooktop and range hoods. A still backplate was installed on the rear wall between the cooktop and range hood for safety.

During experiments, the windows across the top 173 cm of the south wall were covered by horizontal blinds, which were angled to reduce direct sunlight while allowing the room to be lit naturally during daylight hours.

Figure S1. Photo of the cooking area showing the structure in the cooking area, storage structure, and cart.

2 Standard operating procedure of cooking procedure

2.1 Preparation

- Weigh 4L water (22±2 °C) and put in the 11in Stock Pot
- Weigh a full bag of impossible meat without bag (440±20g) and split into equally two parts, each part will be 220±10g

- Weigh 1 tsp salt (5g)
- Weigh 2 tsp olive oil (10g)
- Weigh 1 bottle of tomato sauce into the jar (660±40g)
- Weigh 5 tsp corn oil (20g)

2.2 Boil water in 11in Stock Pot

- Right rear gas burner or induction element with max heat setting (4.4slpm methane) on gas and L7 (~1500W) on Induction
- Add 4L water into the pot and 5g salt
- Heating with lid for ~19 min until boiling

2.3 Sauté meat and simmer sauce in 2 Qt. sauce pot (while boiling the water)

- Weigh the small pot
- Add 10g olive oil to the small pot. Pre-heat pot 30 seconds on medium heat (gas 2.4 slpm methane) or L6 (induction, ~650W) on left front burner or induction element
- Place half bag Beyond burger (220±10g) into pan
- Cook 6 min without lid, keep stirring
- When the oil is dry and the meat is a little sticky to the bottom of the pot, weigh the remaining food in the pot. The food remaining in the pot should be 180±10g, the net loss of the food and oil at the beginning should be 50 ±10g. If not the range, keep cooking for another minute
- Take a picture of the meat in the pan before adding the sauce
- Add 1 jar pasta sauce (660±40g), bring to boil (~9min ~7min). Stir occasionally to make sure meat doesn't stick to the bottom
- Weigh the remaining food in the pot
- Immediately cover, turn off heat, move pot to rear simmer gas burner or induction element. keep on L2/lowest gas setting. No heat.

2.4 Boil pasta in 11in Stock Pot

- Add 450±10g (1 pound) semolina wheat regular-sized spaghetti
- Cook pasta (lid-off) for 9 minutes on high (4.4slpm methane) or L7 (1500W)

2.5 Stir Fry Broccoli while pasta cooks

- Weigh the pan
- Preheat the 9 inch fry pan with 20g corn oil on left front gas burner or induction element:

- high (3.5slpm) for 30sec
- L8 (~1500W) for 20sec

- Add 280±10 g frozen broccoli florets
- Stir fry. with constant stirring
  - gas on high (3.5 slpm) for 6 min
  - induction on L8 (1500W) for 2 min and L7 (750W) for rest 4 min
- When the broccoli is soft, and oil is dry, weigh the remaining in the pan, should be 250±10 g. The net loss of the food and oil in the pan should be 50±10 g.
- Take pictures of what's left in the pan of the broccoli
- Turn off power to the left front and back gas burner or induction element. Wait the pasta to be ready

2.6 Mixing

- Drain pasta and return to 11 qt pot
- Weigh pasta after absorbed water, an ideal weight should be 1100±100g
- pour sauce on pasta then add broccoli, mixing for 30 sec
- Place lid on and begin decay period

2.7 Equipment and Supply List

- IKEA 365+ (404.842.70) 11 Qt.Stock Pot stainless steel (11 in)
- IKEA 365+ (404.842.32) 2 Qt. Sauce Pot stainless steel (7 in)
- IKEA 365+ (504.842.41) Fry pan with non-stick coating (9 in)
- Empava Induction 4-element cooktop (Empv-30ec02)
- Gas cooktop: Whirlpool Cooktop Model (W3CG3014XB)
- Scale: Mettler PJ4000; Mettler-Toledo LLC

3 Equivalent cooking method design by matching power input and net food mass loss

The intention of the experiments was to compare cooking on gas and induction cooktops using cooking procedures that were as equivalent as possible. A key aspect of equivalent cooking is similar heat delivery to the contents of each pot or pan. This was accomplished through trial experiments with various settings of the gas and induction elements to identify those that achieved similar heating of measured quantities of water in each pot or pan, for the specific burners that were used. In these tests, we found that a fuel delivery rate of 4.4 standard liters per minute (SLPM) of methane to the back right gas burner resulted in four liters of water taking ~19 min to reach boiling temperature in the 11-inch stock pot without a lid. The same heating rate was achieved on the back right (largest) induction element at power level 7 (~1500W). Similarly, we found that one liter of water in the small pot on the left front burner took approximately the same amount of time to reach boiling temperature when operated with 2.4 SLPM methane flow or level 6 on the left front induction element (~640W). To match the power inputs for pan frying on the same burner, we found that it took 4.5 minutes of methane flow at 3.7SLPM for 500 mL water to reach boiling in the uncovered pan. A similar heat transfer rate with the induction element in that cooktop location was achieved with the heating time split between L8 (~1500W) and L7 (~750W), to achieve an average heating rate of about 1200 W.

Secondly, we tried to match up the mass loss of the ingredients during the cooking process between the two burners to have the food cooked at a similar level. For frying the meat in the pot, we used 2.4 SLMP methane floor on the gas burner and L6 on induction to cook 220±10g the "meat" for 6 min; the net loss of the food in the pot was within a similar range (50±10g). Similarly, for pan-frying of broccoli, after 6 min cooking of 280±10g frozen broccoli florets on both burners with the same power input, the net loss of the food in the pan was in a similar range (50±10g).

4 Details of each cooking test

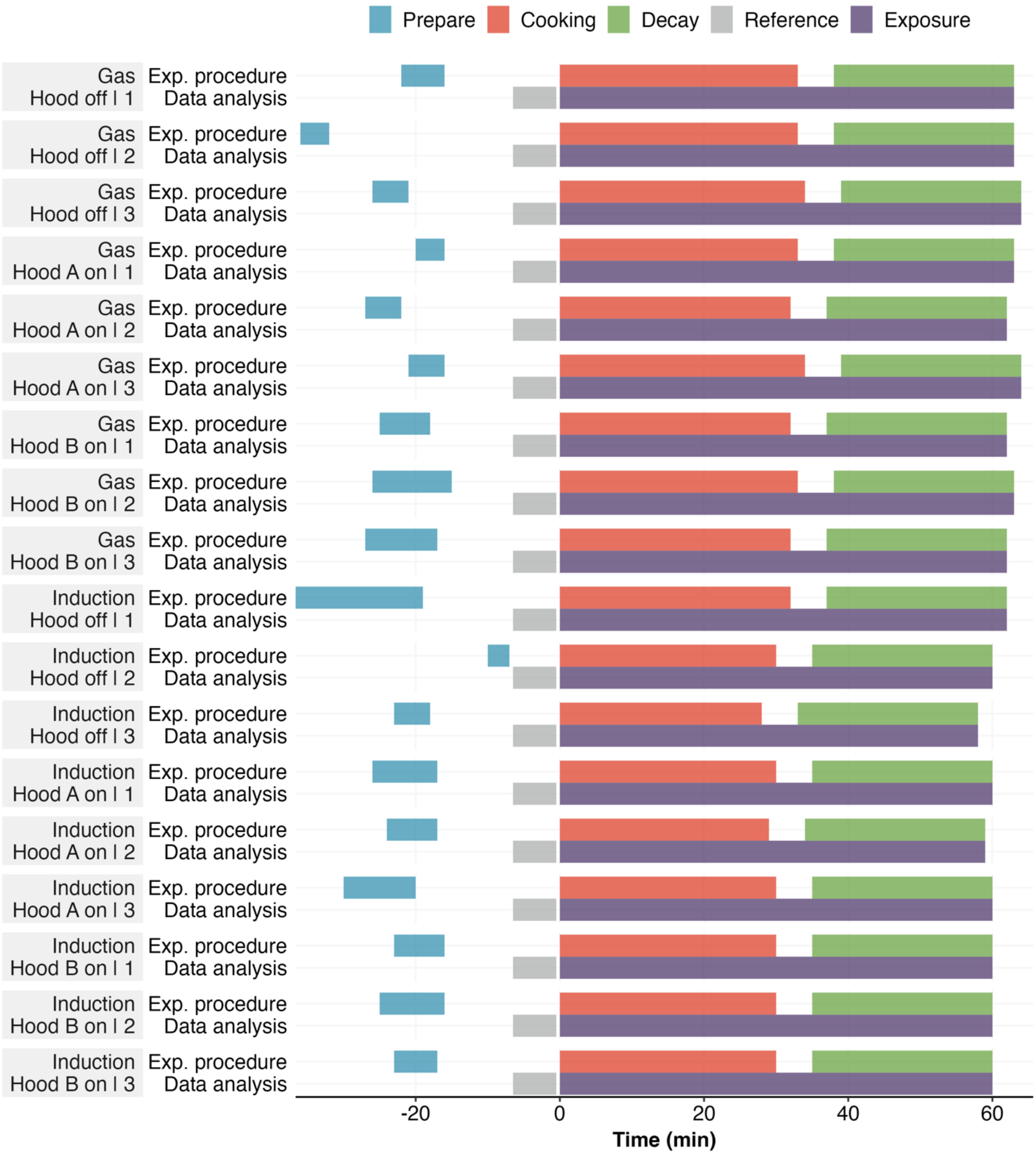

Figure S2. Experiment and data analysis periods for each test.

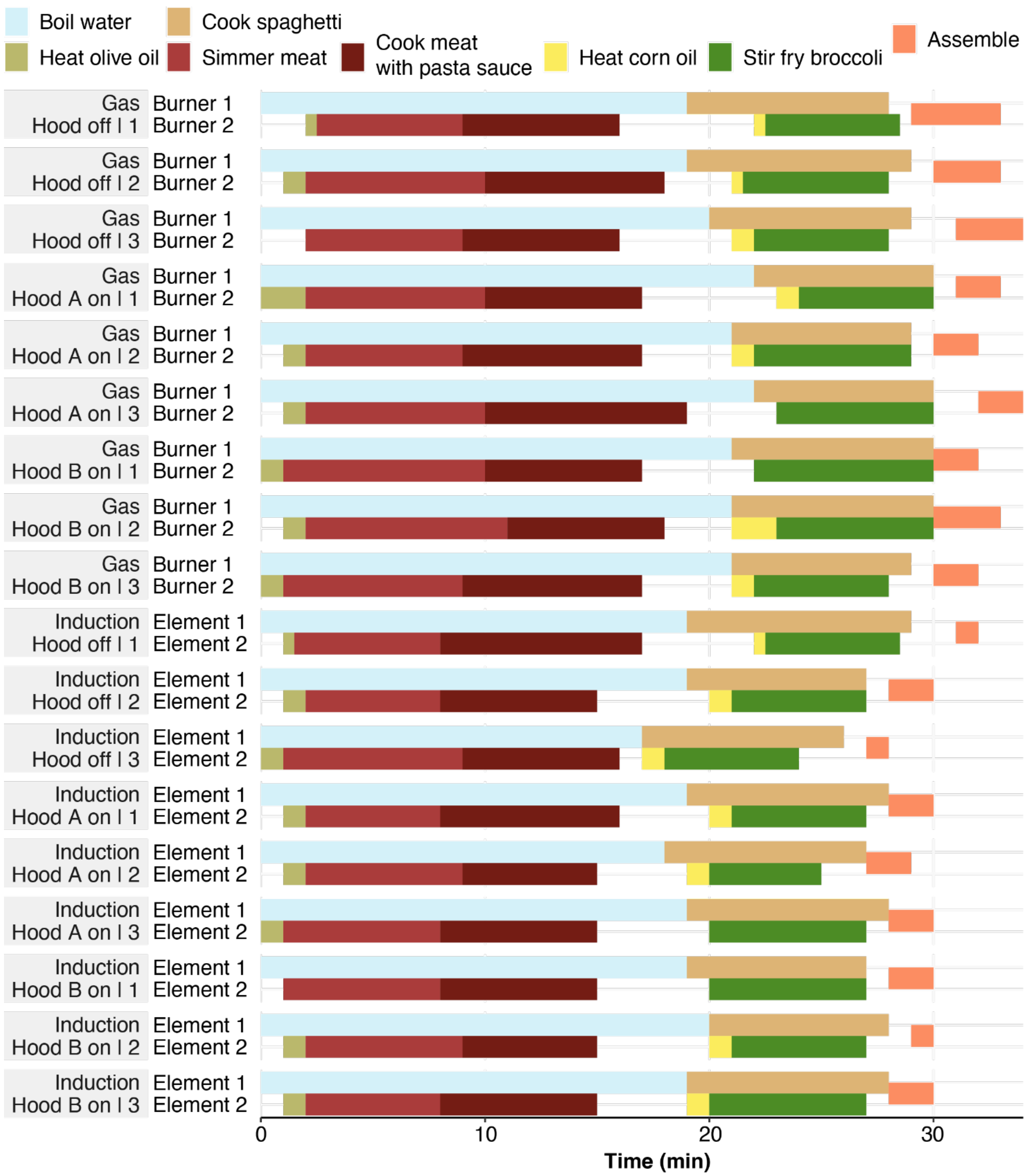

Figure S3. Cooking procedures for each test.

5 Mixed effect model

Assuming $\overline{C_e}(i,j,k)$ represents the averaged exposure concentration, where:

i indexes the cooktop type (i = 1 for gas, i = 2 for induction),

j indexes the range hood (j = 0 for no hood, j = 1 for Hood A, j = 2 for Hood B),

k indexes the measurement within each combination of burner type and range hood (i.e., three repeats).

The mixed-effects model can be described by the following equation:

$$\overline{C_e}(i,j,k) = \beta_0 + \beta_1 X_i + \mu_j + \epsilon_{ijk}$$

Where:

- $\overline{C_e}(i,j,k)$ is the pollutant concentration.
- β_0 is the overall intercept (mean concentration for the reference group, which is the gas burner without a range hood).
- β_1 is the fixed effect coefficient for the cooktop type (X_i), representing the difference in mean concentration between induction and gas cooktops. X_i = 0 for gas burners and X_i = 1 for induction elements.
- μ_j is the random effect associated with the j^{th} range hood, assumed to be normally distributed with mean 0 and variance σ_u^2, capturing the variability in concentration due to different range hood conditions. This is where j = 1 represents the baseline (no hood) condition, with j = 2, 3 for hoods A and B, respectively.
- ϵ_{ijk} is the residual error term, capturing the measurement error and other unexplained variability, assumed to be normally distributed with mean 0 and variance σ_ϵ^2.

The percentage change when switching from gas to induction elements is given by:

$$\eta = \left(\frac{\beta_1}{\beta_0}\right) \times 100$$

6 Additional results

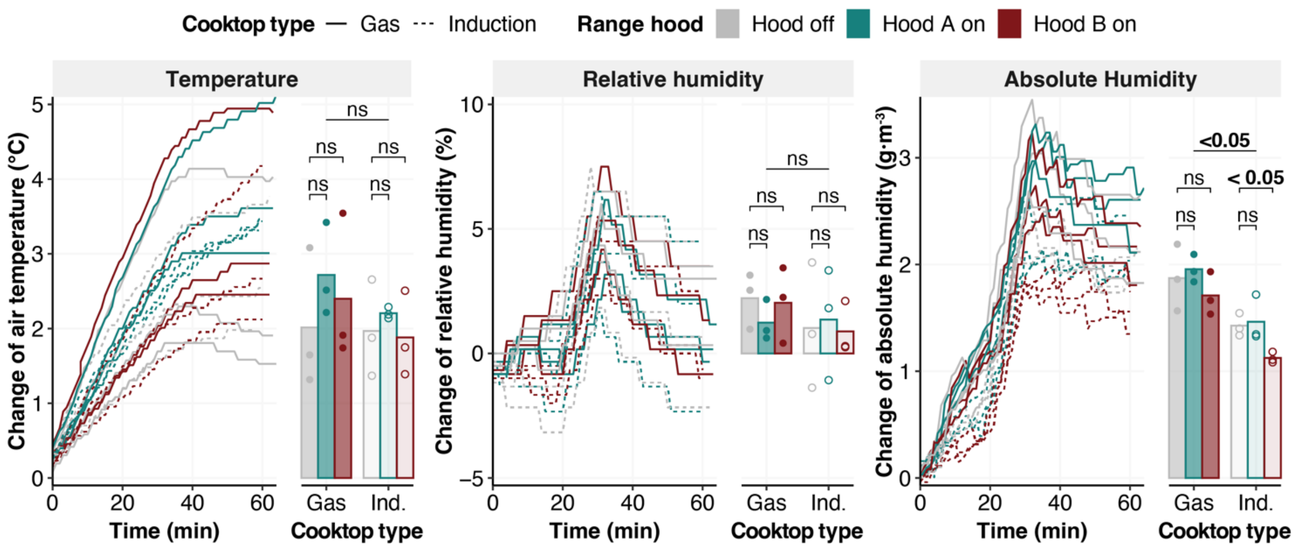

Figure S4. Time-resolved and averaged changes of temperature, relative humidity, and absolute humidity observed during gas and induction cooking, under three range hood conditions. Each solid or hollow point in the figure represents the average of the delta values measured during the exposure period for each experiment.

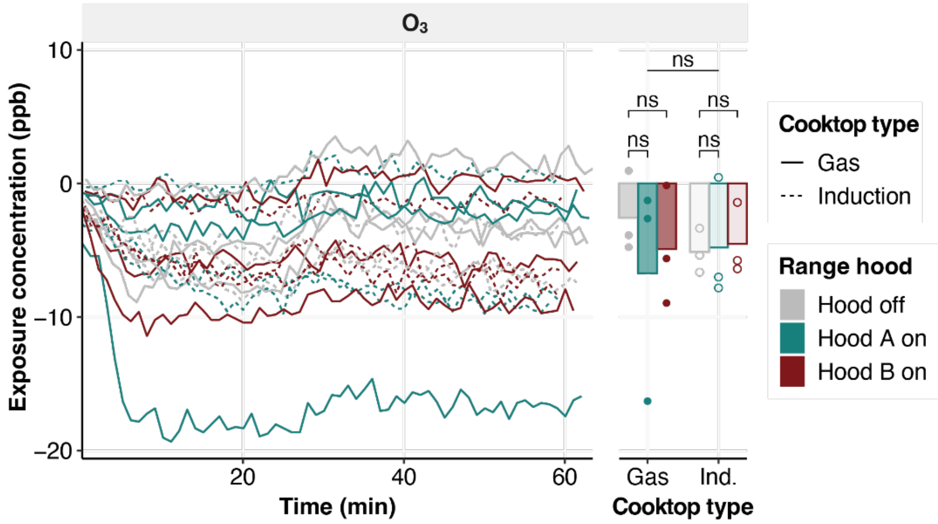

Figure S5. Time-resolved and averaged exposure concentrations of O_3 during gas and induction cooking under three range hood conditions. Each solid or hollow point represents the average net exposure concentration during the exposure period of each experiment.

Table S1. Summary averaged and peak concentrations of UFPs, $PM_{2.5}$, and PM_{10} of all the tests based on data from FMPS + APS.

Range hood	Repeat ID	**UFP** ($\#\cdot10^4\cdot cm^{-3}$)				**$PM_{2.5}$** ($\mu g\cdot m^{-3}$)				**PM_{10}** ($\mu g\cdot m^{-3}$)			
		Gas		Induction		Gas		Induction		Gas		Induction	
		Avg	Peak	Avg	Peak	Avg	Peak	Avg	Peak	Avg	Peak	Avg	Peak
Hood off	1	38.0	117.1	0.9	2.0	18.6	43.6	26.6	57.5	29.4	94.9	59.1	200.4
	2	37.4	95.8	0.7	1.5	11.5	24.9	20.4	43.8	19.2	54.7	43.2	136.1
	3	40.2	100.0	0.4	0.9	9.6	20.5	10.4	20.3	12.2	35.4	21.6	59.1
	Mean	38.5	104.3	0.7	1.5	13.2	29.7	19.1	40.6	20.3	61.7	41.3	131.9
	SD	1.5	11.3	0.2	0.5	4.7	12.3	8.2	18.8	8.6	30.4	18.8	70.7
Hood A on	1	15.4	62.0	0.2	0.4	5.9	14.6	3.7	8.6	6.0	17.6	5.3	18.5
	2	8.6	25.6	0.3	0.7	2.3	5.1	7.1	16.5	2.4	7.1	9.9	35.0
	3	15.9	47.6	0.6	1.5	4.0	9.3	10.9	26.4	3.7	10.5	15.7	57.9
	Mean	13.3	45.1	0.4	0.9	4.1	9.7	7.3	17.2	4.1	11.7	10.3	37.2
	SD	4.1	18.4	0.2	0.6	1.8	4.8	3.6	8.9	1.8	5.3	5.2	19.8
Hood B on	1	12.2	33.8	0.2	0.6	2.0	4.4	3.7	9.9	1.8	5.9	5.2	20.5
	2	15.6	50.2	0.7	2.0	3.3	9.3	14.0	39.8	3.1	11.3	29.4	143.7
	3	15.0	46.8	0.1	0.2	3.9	9.8	1.9	5.2	4.8	14.0	2.6	9.5
	Mean	14.3	43.6	0.3	0.9	3.1	7.8	6.6	18.3	3.3	10.4	12.4	57.9
	SD	1.8	8.6	0.3	0.9	1.0	2.9	6.5	18.8	1.5	4.2	14.8	74.5

Table S2. Result summary of the mixed effect model based on the data from FMPS+APS.

	β_0 [SE]	β_1 [SE]	p-value for β_1	μ_1	μ_2	μ_3	σ_u^2	σ_ϵ^2	η (%)
UFP	2.2e+05 [4.5e+04]	-2.2e+05 [3.2e+04]	9.2e-06	7.1e+04	-3.8e+04	-3.4e+04	4.5e+09	4.6e+09	-97.9
$PM_{2.5}$	6.8 [3.8]	4.2 [2.2]	0.08	6.6	-2.9	-3.7	36.5	21.7	61.9
PM_{10}	9.2 [8.1]	12.1 [5.0]	0.03	13.9	-7.3	-6.7	162.2	110.3	132.0

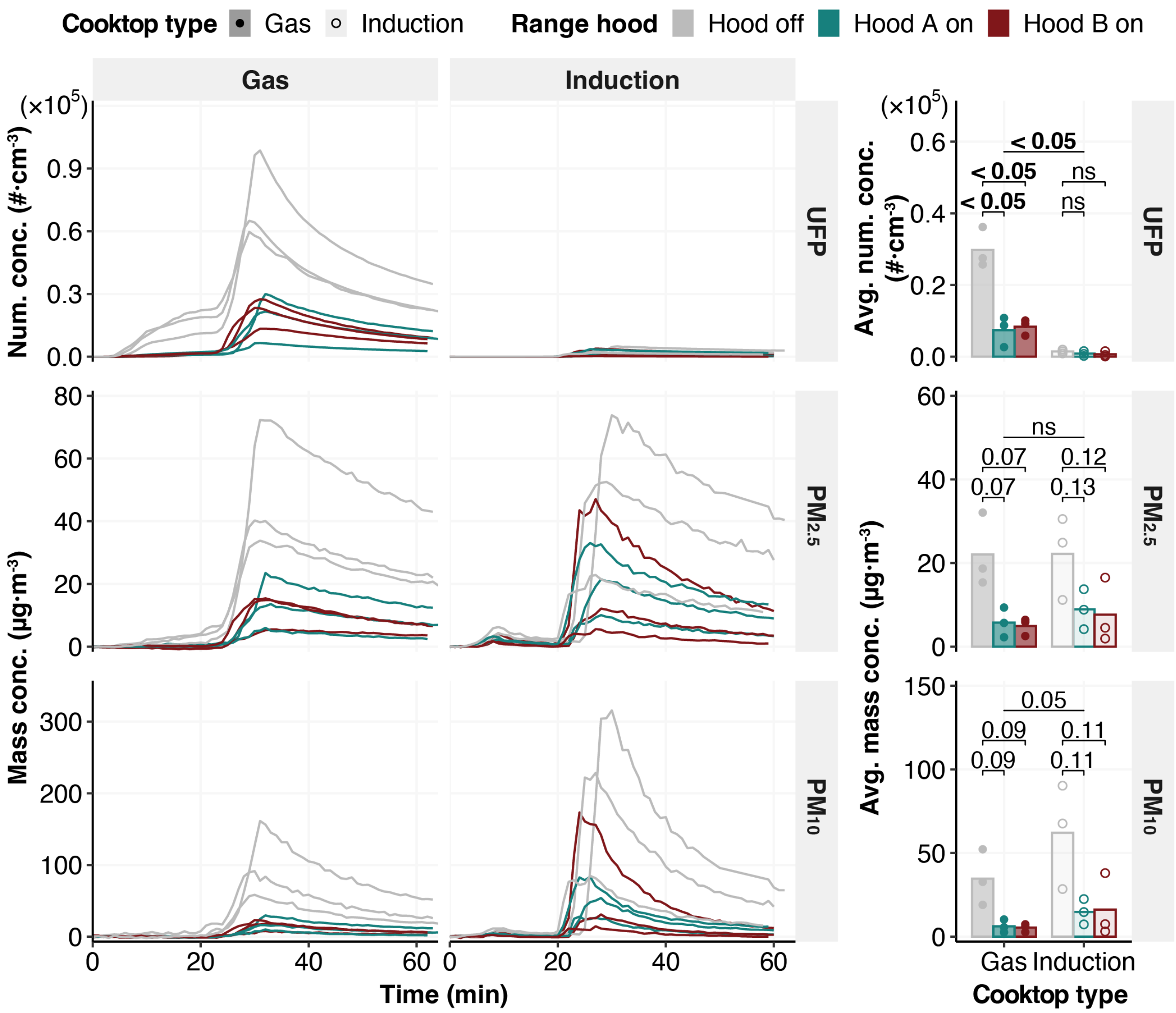

Figure S6. Based on data from Mini-WRAS, time-resolved (left) and time-averaged (columns at right) exposure concentrations of UFPs, $PM_{2.5}$, and PM_{10} during gas and induction cooking under three range hood conditions. Each solid or hollow point represents the average net exposure concentration during the exposure period of each experiment.

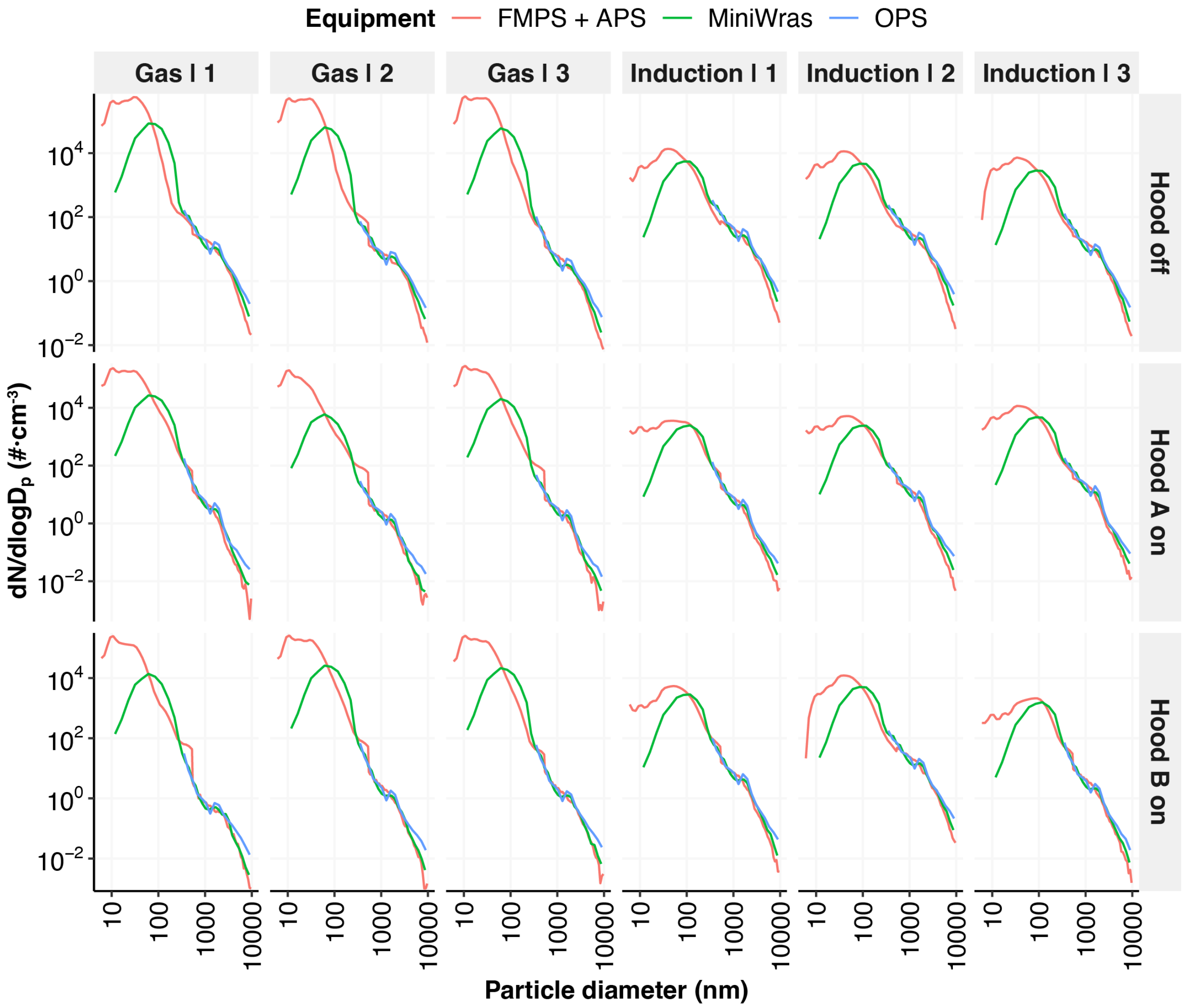

Figure S7. The number-based size distribution of particles measured by different instruments averaged during the exposure periods.

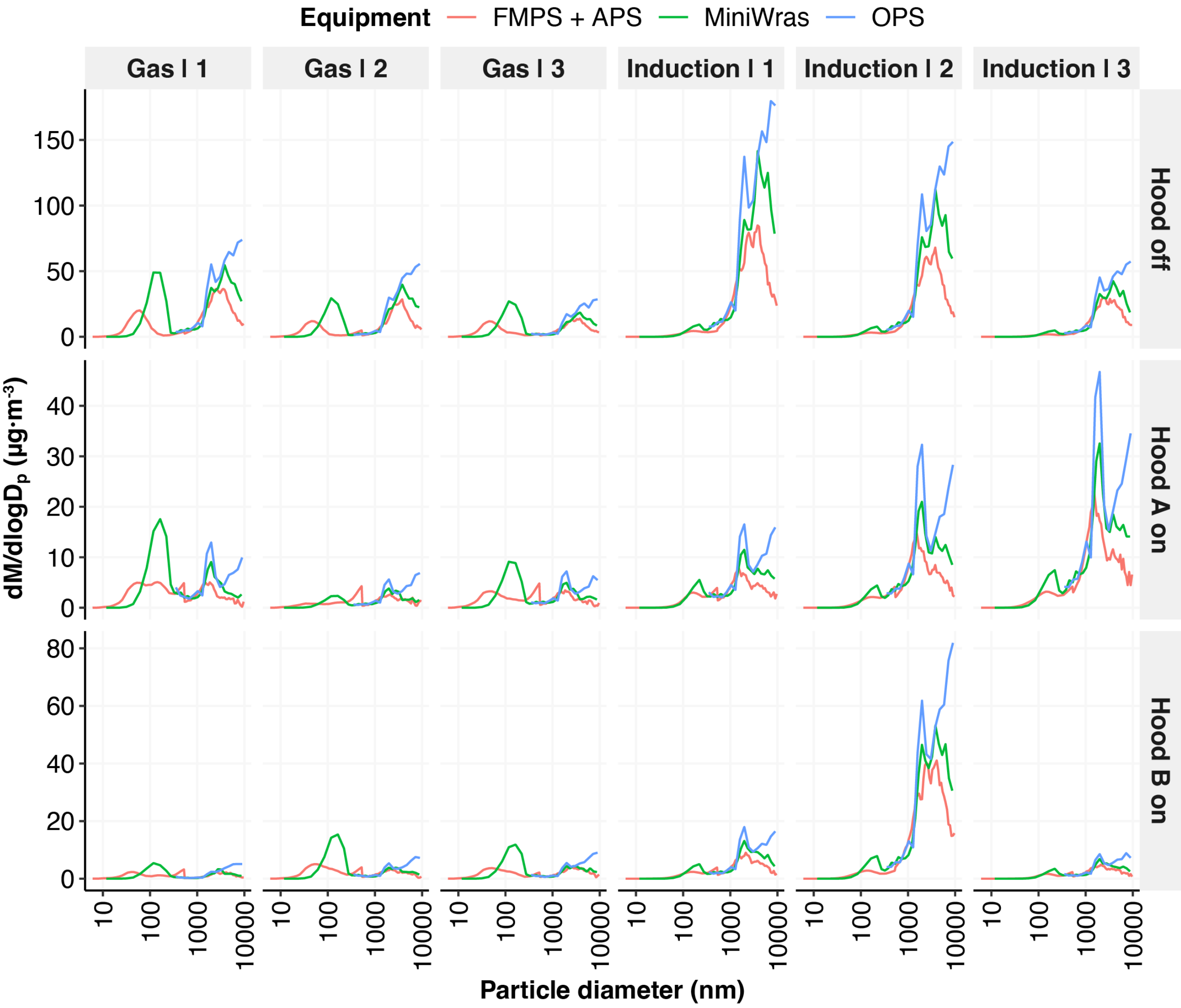

Figure S8. The number-based size distribution of particles measured by different instruments averaged during the exposure periods.

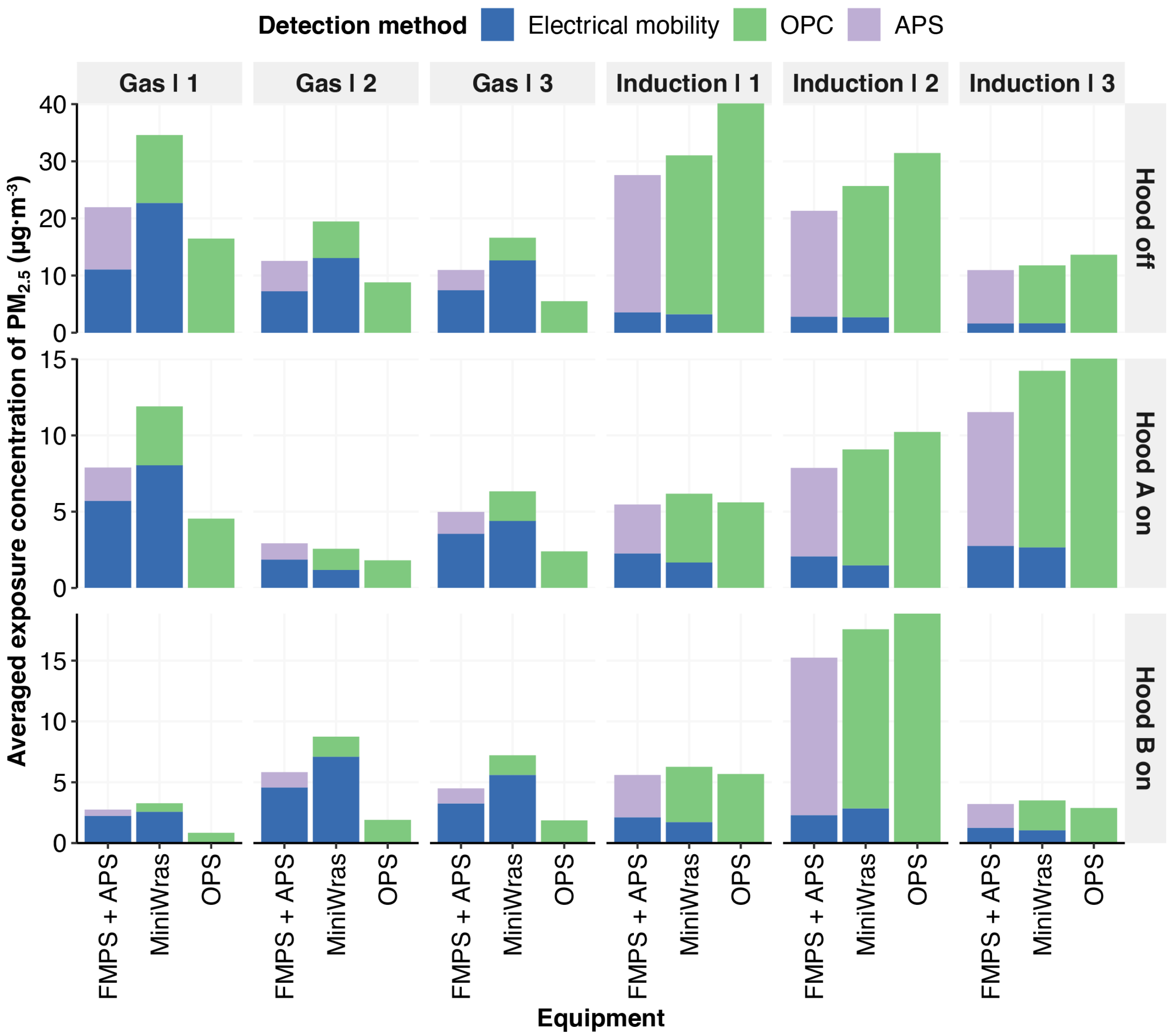

Figure S9. $PM_{2.5}$ concentrations measured by different instruments.